MODEL WORKSHOP ON STRATEGIES FOR COUPLING HIGHER AND LOWER TROPHIC LEVEL MARINE ECOSYSTEM MODELS

(Co-convenors: Michio J. Kishi and Bernard A. Megrey)

Introduction

A variety of models have been used to describe lower trophic level (LTL) and higher trophic level (HTL) components of North Pacific ecosystems. In order to facilitate comparisons of model results among areas, the goal of the MODEL Task Team for the next few years is to adapt a prototype LTL model developed at the workshop held in Nemuro, Japan, in January 2000, and to apply it to basin and regional scale ecosystems in the North Pacific. These activities will require coordination with BASS, REX, and MONITOR Task Teams. The Nemuro Workshop focused on the development and parameterization of a LTL model to PICES regional ecosystems, and began discussions about ways to link HTL models to LTL models. The follow-up Hakodate Workshop described in this report was intended to extend the initial discussion that began in Nemuro, and to develop viable strategies for this important linkage.

The following summary of the Task Team discussions from the Hakodate Workshop outlines some important factors which determine how LTL production flows to HTL predators, and how much of this energy is transformed into HTL production. Many of the factors and processes mentioned below should be included, either explicitly or implicitly, in an HTL model. The output of the coupled model should also be analyzed to ensure that it is able to reproduce reasonable production/biomass and consumption/biomass ratios, and ecotrophic efficiencies.

Goals and objectives of the workshop

The goals of the workshop were to:

1. Collectively identify viable strategies for linking the NEMURO LTL (Fig. 1) model to HTL models of the North Pacific ecosystem at the regional and basin scales of interest to BASS and REX.
2. Develop strategies for integrating different time/space scales and size spectra from various models.
3. Find areas of mutual interest where MODEL could interact with other CCCC Task Teams, especially REX and BASS.
4. Achieve broad synthesis through modeling which will lead to global understanding of the response of marine ecosystems to global climate change.
5. Discuss strategies for simulating variability in populations of fish and zooplankton, to evaluate the cause of this variability, and to identify approaches that will ultimately permit the development of a predictive capability.
6. Discuss how to best link LTL and HTL marine ecosystem models, regional circulation models, and how to best incorporate these unified models into JGOFS models and the CCCC Program.

Participants, venue and schedule

The workshop was held at the Future University in Hakodate, Japan, during the PICES Ninth Annual Meeting in October 2000. Participants (MODEL Endnote 1) consisted of LTL and HTL modelers and individuals with knowledge about key data sets in each selected region and activity within that region.

The workshop schedule (MODEL Endnote 2) consisted of a half-day CCCC plenary session held jointly with other CCCC Task Teams. This was followed by a full-day MODEL Workshop. The final afternoon consisted of a wrap-up CCCC plenary session. During PICES X there were several impromptu meetings between MODEL and BASS, and between MODEL and REX.

The following section contains abstracts, extended abstracts, and fully prepared reports presented at the workshop. The reports are organized by author according to the workshop schedule. The author in bold font made the presentation. Model versions referenced in these reports are described in Megrey *et al.* (2000).

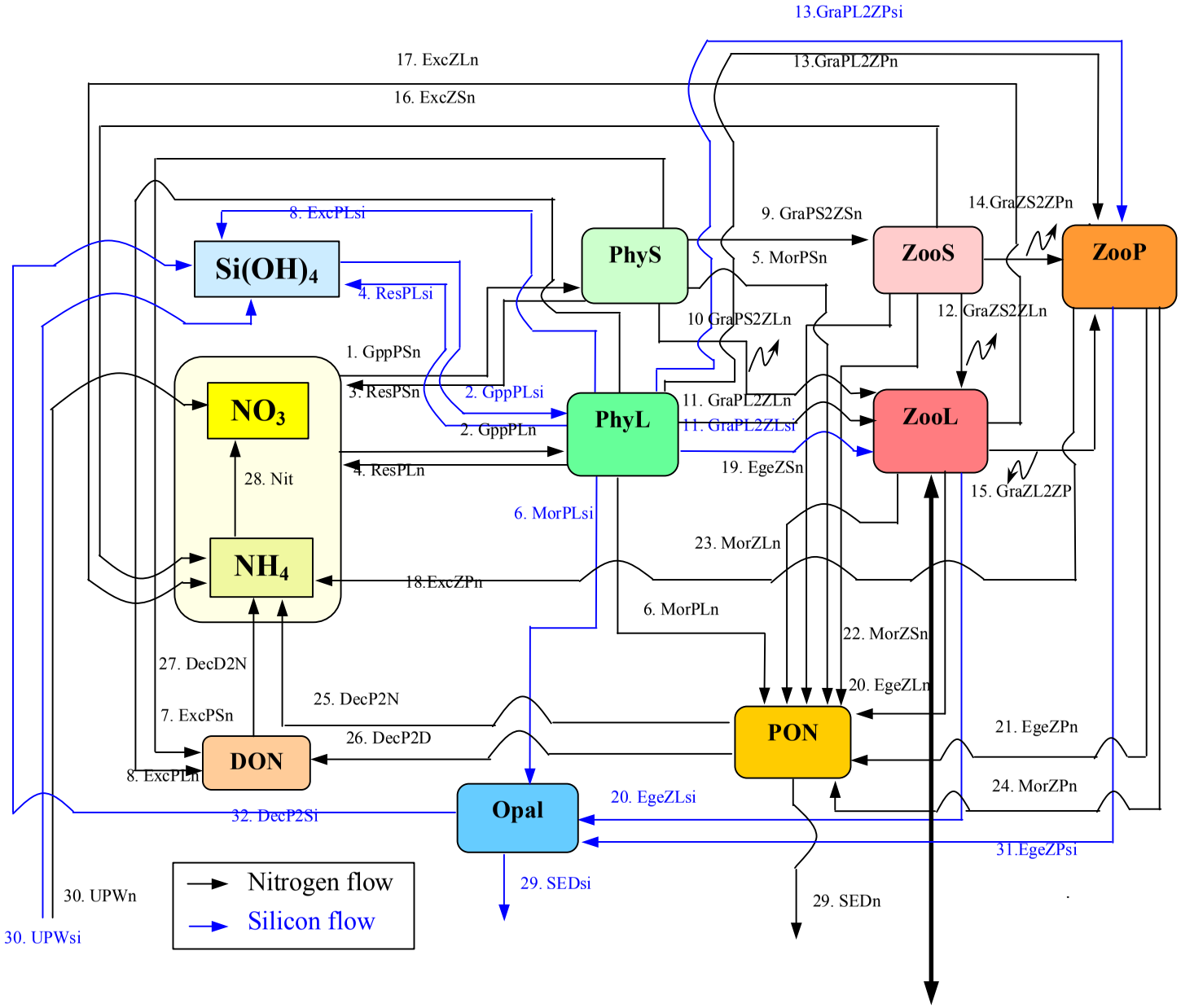

Fig. 1 NEMURO – A PICES/CCCC prototype lower trophic level marine ecosystem model of the North Pacific Ocean. The dark arrow indicates diel vertical migration by large zooplankton (ZooL).

Strategies for coupling upper and lower trophic levels in ecosystem models

Kenneth A. Rose
Coastal Fisheries Institute & Department of Oceanography and Coastal Sciences, Louisiana State University, Baton Rouge, LA 70803, U.S.A. E-mail: karose@lsu.edu

Ecological issues have become complex, with increasing emphasis being placed on ecosystem considerations. Anthropogenic stresses on the ecosystem, such as global climate change, require a whole-system approach to adequately account for both the direct and indirect effects. Yet, despite great effort, we have had great difficulty in quantitatively understanding the relationships between habitat and fish population dynamics (Rose 2000). Previous efforts of the PICES MODEL Task Team have involved development of a lower trophic level simulation model (NEMURO) that tracks nitrogen, phytoplankton, and zooplankton (NPZ). In my presentation, I focus on the issues and strategies related to coupling upper trophic levels to lower trophic models, such as the NEMURO NPZ model. I also present three examples that illustrate these issues and strategies. I conclude with some general comments related to coupling upper and trophic levels in dynamic models.

There are five general issues that must be considered when coupling upper and lower trophic levels. These issues are: (1) spatial and temporal scales, (2) biological scale, (3) site-specificity, (4) feedbacks, and (5) specification of the question. Good models are properly scaled to address the question of interest.

The temporal scale is defined by the time step of the model and the duration of the simulations. The spatial scale is defined by the grain (finest grid size) and extent (geographic area being modeled). The processes controlling nitrogen, phytoplankton and zooplankton operate on different time and space scales than those important to fish, birds and mammals. Most everyone would agree that a 90-second timestep on cm-scale spatial grid is not appropriate to simulate long-term fish population dynamics. The optimal temporal and spatial scales in a model are determined by the properties of the important processes, the availability of data, and the questions to be addressed. Unfortunately, there are no general rules for knowing whether the optimal scales are being represented in a particular model.

The second issue of specifying the biological scale is related to determining the optimal temporal and spatial scales. When modeling upper trophic levels, a fundamental decision is whether the question can be addressed with partial or full life cycle predictions. Partial life cycle predictions might be survival and growth during a particular life stage or period of time. Full life cycle simulations allow for multiple generations to be simulated and for long-term predictions. Developing models that permit full life cycle simulations is a much more difficult and labor-intensive effort. New issues, such as long-term population stability, become important. Population models that do not include negative feedbacks (density-dependence) have only two possible solutions, either extinction or populations going to infinity. Neither of these ultimate solutions is realistic for full life cycle situations; yet, the most difficult aspect of full life cycle modeling is specifying the density-dependent (negative feedback) relationships.

The third issue of site-specificity also greatly influences the effort involved with model development and validation, and the appropriate way to interpret predictions. Models can be developed that attempt to simulate the population in an actual geographic area for specific time periods. Such models require extensive data to account for the nuances of the particular population and location and are more involved to develop, but result in higher confidence in site-specific predictions and results that are easy to relate to resource management. The alternative approach is to develop models that do not claim to simulate a particular location and time period, but rather, simulate a taxa like the species of interest in environments representative of the area of interest. Such models are usually easier to

configure because data can be borrowed from related species and from nearby or similar geographic areas. The disadvantages to such representative models are that we have low confidence in their site-specific predictions and their interpretation focuses on patterns rather than magnitude. The relative merits of the site-specific versus representative models depend on the resolution required to address the question of interest.

The fourth issue is how to represent feedbacks in coupled lower and upper trophic level models. Model coupling is simplified if the effects between trophic levels can be assumed to be bottom-up. This allows the lower trophic model to be run separately from the upper trophic level model. If the dynamics of the upper trophic levels affect the dynamics of the lower trophic levels, then simultaneous solution of both levels are required. Another type of important feedback is the negative feedbacks that act to stabilize population dynamics. Accurate prediction of the dynamics of upper trophic levels requires understanding of the density-dependent feedbacks that operate to keep populations within certain numerical bounds. Representing these feedbacks in upper trophic models can be difficult and, at times, controversial. The shape of spawner-recruit curves assumed in fish population dynamics models is a good example. Such feedbacks determine the response of populations and communities to stressors, and ultimately determine the resilience of the population and the magnitude of harvest that is sustainable.

The fifth, and perhaps most important, issue related to coupling upper and trophic level models is the specification of the question to be addressed. The question of interest must be clearly specified, preferably stated as an hypothesis or family of hypotheses. Otherwise, one is assured of developing an improperly scaled model with the wrong structure, inputs, and outputs. Treating the modeling effort as an experiment with hypotheses and experimental design can avoid many of the problems with inappropriate models. A saying with some merit is that "there are no bad models, just bad model applications".

Two commonly used modeling approaches for upper trophic levels are matrix projection modeling and individual-based modeling. Matrix projection modeling has the advantages of using readily available data on growth, mortality, and reproduction, and well-known mathematical solution (eigenvalue analysis) methods. The disadvantages to the matrix approach are that adding stochasticity and density-dependence often limits the ability for mathematical analysis; density-dependence is represented with aggregate, difficult-to-measure, relationships; all individuals in a life stage are treated as identical; and only a few discrete spatial regions can be represented.

Two general approaches to individual-based modeling are the p-state and i-state methods. The *p*-state approach follows probability distributions of individuals with partial differential equations. The *i*-state approach simulates individuals as discrete units, following thousands of such individuals in simulations. DeAngelis *et al*. (1993) showed that both approaches yield very similar predictions when formulated from the same information. The *p*-state approach is mathematically elegant, while the *i*-state approach is more flexible allowing for greater biological realism. I focus on the *i*-state approach in this presentation. The *i*-state approach is conceptually appealing. The individual is the evolutionary unit in nature, and summing over individuals yields population level behavior. The *i*-state individual-based approach addresses some of the disadvantages of the matrix projection approach. Representation of episodic effects, local interactions, and movement of individuals is relatively easy. Also, the difficult-to-specify density-dependent relation-ships inherent in the matrix approach become emergent properties of the rules imposed on individuals. The disadvantages to the *i*-state individual-based approach are that it is data hungry, computationally intensive, sometimes difficult to validate at the individual level, and due to lack of data, individuals are often assigned the same average values.

I use three examples of upper trophic levels being coupled to lower trophic level or physical models

to illustrate these five issues, and to also illustrate the use of matrix and individual-based modeling. These examples are: walleye pollock, striped bass, and northern anchovy. Hinckley (1999) embedded individual fish as particles into a 3-D hydrodynamics model, and then allowed the individuals to encounter prey via a coupled NPZ model. The model was site-specific, focused on young-of-the-year (YOY) life stages, and was designed to understand recruitment variability. Model results illustrated the benefits of a Lagrangian approach for modeling of upper trophic levels in spatially-explicit grids.

The second example is a model of striped bass population dynamics (Rose *et al.* in prep.), and illustrates a hard-coupling between upper and lower trophic levels. YOY striped bass were simulated using a detailed, individual-based model. This process-based YOY model was coupled to an age-structured matrix projection model for ages 1 to 17 to permit multigenerational simulations. For the YOY model, San Francisco Bay was divided in four coarse spatial boxes. A spatially-detailed hydrodynamics model was used to simulate particle transport for typical low flow and average flow years. Movement of individuals among the four coarse spatial boxes in the YOY model was based on probability transitions estimated from the hydrodynamic simulations. Predicted spatial distributions of YOY in the four boxes agreed with observed spatial distributions. A set of 30-year simulations showed that no single factor could explain the decline in striped bass, but that the combined effects of the multiple factors resulted in a realistic rate of population decline. One of the most controversial aspects of the entire modeling exercise was the density-dependent survival from age-1 to age-3 assumed in the adult matrix model.

The third example is an individual-based, full life cycle model of northern anchovy in the California Bight (Wang *et al.* 1998). This example illustrates a soft-coupling. Individuals were followed from birth to death in a two box model. Movement was simulated using a set of simple rules that were qualitatively based on measured distributions and transport considerations. Typical zooplankton densities for normal and ENSO years were determined from long-term monitoring data, but could also be thought of spatially-averaged output of a NPZ model. Climate change was simulated by increasing the intensity assumed for ENSO conditions, by increasing the frequency of ENSO years, and both combined. While predicted northern anchovy population abundance in 200-year simulations was generally lower under more intense and more frequent ENSO conditions, there were also periods of 10 or more years in which predicted abundances were similar to baseline conditions.

In summary, I presented a brief (and biased) view of how to couple upper trophic levels to lower trophic levels in ecosystem models. The *lessons learned* were:

(1) Highly site-specific models allow easy interpretation of predictions but require a large effort and have questionable generality;

(2) Avoid reliance on intuition, as responses are often not proportional to the magnitude of changes imposed and interactive effects among multiple, time-varying factors are the norm rather than the exception;

(3) Maintain a keen awareness of the capabilities of the model to ensure the formulations are appropriate for addressing the specific questions of interest,

(4) Be flexible and willing to use a suite of models, with each tailored to a particular problem and realize that the obvious way to couple trophic levels may not be the optimal approach; and

(5) Clearly define the question of interest as a hypothesis and then tailor the model or models to the particular problem.

Summary of Nemuro 2000: An international workshop to develop a prototype lower trophic level ecosystem model for comparison of different marine ecosystems in the North Pacific

Bernard A. Megrey[1], Michio J. Kishi[2], Daniel M. Ware[3] and Makoto Kashiwai[4]

[1] National Marine Fisheries Service, Alaska Fisheries Science Center, 7600 Sand Point Way NE, Seattle, WA 98115, U.S.A. E-mail: bern.megrey@noaa.gov
[2] Hokkaido University, Graduate School of Fisheries Sciences, Hakodate, Hokkaido, Japan. 041-8611 E-mail: kishi@coast0.fish.hokudai.ac.jp
[3] Adjunct-Professor, Department of Earth and Ocean Sciences, University of British Columbia. Mailing Address: 3674 Planta Road, Nanaimo, B.C., Canada. V9T 1M2 E-mail: mandd@island.net
[4] Hokkaido National Fisheries Research Institute, Katsurakoi 116, Kushiro, Hokkaido, Japan. 085-0802 E-mail: kashiwai@hnf.affrc.go.jp

An ecosystem model with 11 compartments was developed in order to describe primary and secondary production in the Northern Pacific Ocean. This model was made by the request of the PICES/GLOBEC CCCC Program. Model equations describe the interactions of nitrate, ammonium, silicate, two phytoplankton size fractions (tentatively, these are diatoms and flagellates), three zooplankton size fractions (tentatively, microzooplankton, copepods, and predatory zooplankton), as well as nutrient kinetics. Formulations for the biological processes are based primarily upon process equations presented in Kawamiya *et al.* (1995). A 1-D physical-biological coupled model including a mixed layer closure model (1-D NPZ model) is used to simulate time dependent features of the ecosystem at three locations: Ocean Station P, Station A7 of the Akkeshi line off Hokkaido Island, Japan, and a region in the southeast Bering Sea. Time series of biological dynamics from the biological model as well as time-depth distributions of nutrient and plankton obtained from the 1-D NPZ model for three regions in the North Pacific are compared. This presentation summarized the work and accomplishments of the PICES CCCC/MODEL Task Team Workshop, held in Nemuro, Japan, in January 2000 (see PICES Scientific Report No. 15, and Megrey *et al*. 2000, and for details).

Sensitivity analysis on NEMURO

Michio J. Kishi and Hiroshi Kuroda
Graduate School of Fisheries Sciences, Hokkaido University, Hakodate, Hokkaido, Japan. 041-8611 E-mail: kishi@coast0.fish.hokudai.ac.jp

A sensitivity analysis was performed on the NEMURO/FORTRAN Box model using the Monte Carlo analysis. The ecological parts of the model were run to calculate the nitrogen-based biomass of each compartment until steady state solutions were obtained. Values of each compartment and ecological parameters were stored to be used as the baseline values around which random perturbations were generated and put into the Monte Carlo error analysis. A Monte Carlo error analysis with 600 individual calculations was made with input parameters and initial values perturbed independently over random error distribution with limits of ± 10% of base line values. Principal component analysis (PCA) was used to reduce the 600 sets of output of biological parameters and initial values. The PCA indicated four factors, which together, explained 22% of the variance in the data space. The first principal component, which was clearly related to photosynthesis of PL, accounted for 10% of the data space variance and included the variables

V_{maxS}, V_{maxL}, and PL, $N0_3$, NH_4. The second principal component was related to the zooplankton state variables, ZL and ZS. Based on this sensitivity analysis, we selected five biological parameters to estimate using data from the A-line (off Hokkaido, Japan - outside Oyashio region) and guessed parameter values. We used the conjugate gradient method (FR method) to get the local minimum of the cost function, which is defined by the squared difference between observed and simulated chlorophyll and NO_3.

The cost function is:

$$f = \sum_{i=1}^{N_1} M_1 (PhySn(i) + PhyLn(i) - chla(i))^2 + \sum_{i=1}^{N_2} M_2 (NO_3(i) - NO_3 dat(i))^2 + \sum_{k=1}^{11} M_k^{/} (C_k(1440) - C_k(0))^2$$

The parameters to be estimated were V_{maxS}, V_{maxL}, λ_P, Mor_{ZP0} and $VD2_{N0}$, and the initial values were:

Group A

V_{maxS} = 0.500	(day^{-1})
V_{maxL} = 0.200	(day^{-1})
λ_P = 1.50E+06	(molN/l)
Mor_{ZP0} = 5.00E+04	(day^{-1})
$VD2_{N0}$ = 2.20E-02	(day^{-1})

However, we were unable to find a stable local minimum with the above first guess. Consequently the following values were used as the first guess:

Group B

V_{maxS} = 1.50	(day^{-1})
V_{maxL} = 0.20	(day^{-1})
λ_P = 1.00E+06	(molN/l)
Mor_{ZP0} = 5.85E+04	(day^{-1})
$VD2_{N0}$ = 5.00E-02	(day^{-1})

The parameter values that minimized the cost function were:

Group C

V_{maxS} = 0.206	(day^{-1})
V_{maxL} = 0.184	(day^{-1})
λ_P = 0.668E+06	(molN/l)
Mor_{ZP0} = 5.224E+04	(day^{-1})
$VD2_{N0}$ = 2.151E-02	(day^{-1})

With these values, we calculated the time dependent features of each compartment of the NEMURO/FORTRAN Box model. Two specific examples are presented in Figures 2 and 3. It is clear the results seem much better if the new assimilated parameter values are used. A more detailed analysis will be done in the future.

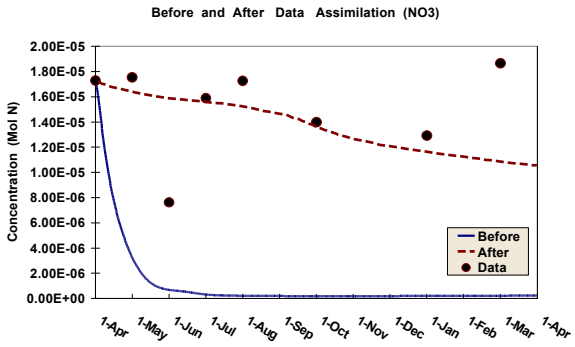

Fig. 2 The time dependent features of NO_3 by the NEMURO/FORTRAN Box model. The blue line shows results with parameter set Group B and the pink line with Group C (assimilated parameters). Dots indicate the mean averaged observed value of the upper 100 m at station A7.

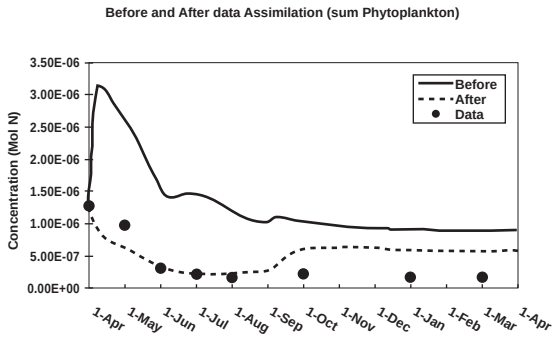

Fig. 3 The time dependent features of PS + PL by the NEMURO/FORTRAN Box model. The blue line shows results with parameter set Group B and the pink line with Group C (assimilated parameters). Dots indicate the mean averaged observed value of the upper 100 m at station A7.

To the physical forcing and the ways of improvements in the NEMURO Model

Vadim V. Navrotsky
Pacific Oceanological Institute, Vladivostok, Russia. 690041 E-mail: navr@online.vladivostok.ru

Supposing we know the behavior of the biological part of an ecosystem with stationary physical conditions, the problem is to define the main physical parameters and the ways of their influence on the ecosystem behavior. In the NEMURO model, the main physical parameter entering almost all equations is temperature, which is calculated with the use of a mixed layer model. Many observations (examples for the northwestern Pacific and Okhotsk Sea are given) show that small-scale fluctuations of the temperature gradient vertical structure (fine-structure FS and microstructure MS) are important as for vertical distribution of plankton, and for its integral biomass. Mechanisms of FS and MS influence on phytoplankton and zooplankton production may be different, but as a first approximation we propose to use an additional coefficient proportional to *rms* of the vertical temperature fluctuations in the layer studied (0-330 m) in all temperature-dependent terms. The values of *rms* can easily be obtained from observations (XBT, for example), and a model is proposed that helps to evaluate them.

Some additional improvements in the model are discussed, including: 1) time-lag in the dependence between zooplankton and phytoplankton concentrations; 2) adjusting averaging scales to the intrinsic (biological) and forced (physical) time scales; 3) interdependence between input parameters; and 4) criteria for comparisons between models and observations.

Summary of extensions to the NEMURO/MATLAB Box Model developed at the Hakodate PICES Meeting

David L. Eslinger[1], Daniel M. Ware[2], **Francisco E. Werner[3]** and Bernard A. Megrey[4]

[1] Coastal Remote Sensing Program, NOAA Coastal Services Center, 2234 South Hobson Avenue, Charleston, SC 29405-2413, U.S.A. E-mail: dave.eslinger@noaa.gov

[2] Adjunct-Professor, Department of Earth and Ocean Sciences, University of British Columbia. Mailing address: 3674 Planta Road, Nanaimo, B.C., Canada. V9T 1M2 E-mail: mandd@island.net

[3] Marine Sciences Department, CB# 3300, University of North Carolina, Chapel Hill, NC 27599-3300, U.S.A. E-mail: cisco@email.unc.edu

[4] National Marine Fisheries Service, Alaska Fisheries Science Center, 7600 Sand Point Way NE, Seattle, WA 98115, U.S.A. E-mail: bern.megrey@noaa.gov

Discussion and extensions to the NEMURO/ MATLAB Box model at the Hakodate Workshop and the months that followed included three main components: development of diagnostics and comparison to observed and literature values, effect of vertical migration by large zooplankton, and the inclusion of an approximation to a microbial loop formulation. Results of these experiments, which are summarized below, are presented for the Station P location.

Diagnostics of NEMURO at Station P

To quantify the results of the NEMURO/ MATLAB Box model at Station P, we developed a series of diagnostic measures including daily production/biomass ratios (P/B) for phytoplankton and zooplankton, and food consumption/biomass ratios (C/B) for small, large and predatory zooplankton and the ecotrophic efficiency (EE), a measure of how much primary production transfers to the zooplankton species. A brief description of the procedures and results is given below.

1. Output for the 8th year from the model was post-processed to calculate a number of variables: daily P/B ratios for phytoplankton and zooplankton, and C/B ratios for small, large and predatory zooplankton and the ecotrophic efficiency.
2. The P/B, C/B and EE are calculated as follows:

NPPS=GppPSn-ResPSn – Net Primary Production for small phytoplankton
NPPL=GppPLn-ResPLn – Net Primary Production for large phytoplankton
NCZS=GraPS2ZSn+GraPL2ZSn – Net Consumption for small zooplankton
NCZL=GraPS2ZLn+GraPL2ZLn+GraZS2ZLn – Net Consumption for large zooplankton
NCZP=GraPL2ZPn+GraZS2ZPn+GraZL2ZPn – Net Consumption for predatory zooplankton
TNPP=NPPS+NPPL – Total Net Primary Production
TGPP=GraPS2ZSn+GraPS2ZLn+GraPL2ZLn+GraPL2ZPn – Total Gross Primary Production
NPZS=NCZS-ExcZSn-EgeZSn – Net Production for small zooplankton
NPZL=NCZL-ExcZLn-EgeZLn – Net Production for large zooplankton
NPZP=NCZP-ExcZPn-EgeZPn – Net Production for predatory zooplankton
P2BPS=NPPS/PS – Production/Biomass Ratio for small phytoplankton
P2BPL=NPPL/PL – Production/Biomass Ratio for large phytoplankton
P2BZS=NPZS/ZS – Production/Biomass Ratio for small zooplankton
P2BZL=NPZL/ZL – Production/Biomass Ratio for large zooplankton
P2BZP=NPZP/ZP – Production/Biomass Ratio for predatory zooplankton
C2BZS=NCZS/ZS – Consumption/Biomass Ratio for small zooplankton
C2BZL=NCZL/ZL – Consumption/Biomass Ratio for large zooplankton
C2BZP=NCZP/ZP – Consumption/Biomass Ratio for predatory zooplankton
EE=TGPP/TNPP – Ecotrophic Efficiency (all zooplankton)
EEZLZP=(TGPP-GraPS2Zsn)/TNPP – EE for large and predatory zooplankton only

Table 1 Results of NEMURO/MATLAB Box model simulations.

Variable	Group	Model Value	Empirical Value	Source
P/B daily P/B annual B mean	PS	0.108-0.636 /d mean = 0.355/d ~ 0.12		
P/B daily P/B annual B mean	PL	0.032-0.212/d mean = 0.116/d ~0.11		
P/B daily P/B annual B mean	ZS	0.081-0.222/d mean = 0.134/d ~0.055		
P/B daily P/B annual B mean	ZL	0.026-0.127/d mean = 0.065/d ~0.055		
P/B daily P/B annual B mean	ZP	0.001-0.015/d mean = 0.007/d ~0.08		
C/B	ZS	0.387-1.06/d mean = 0.639/d		
C/B	ZL	0.124-0.604/d mean = 0.308/d		
C/B	ZP	0.004-0.070/d mean = 0.033/d		

Table 2 Comparison of NEMURO/MATLAB Box model results to empirical estimates.

Variable	Group	P/C	Empirical	Source
P/C	ZS	0.21	0.2-0.3	Straile 1997
P/C	ZL	0.21	0.2-0.3	Straile 1997
P/C	ZP	0.21		

Results

Simulation results (Fig. 4) show that there is a small spring bloom of large phytoplankton (PL) (which peaked at a level of about 3× the average biomass around time year 8.2 (or day 73 or March 13)). This bloom is an artifact of the "box" nature of the model. The addition of a process to "activate" grazing by the large zooplankton (ZL) when the large phytoplankton begin to bloom is discussed later in this report.

Figure 5 shows the P/B, C/B, and P/C (production/ consumption) ratios. Additional model result summaries are presented in Tables 1 and 2 from the model output for year 8. In this case, the P/B ratio= specific growth rate (daily), the P/C ratio= growth efficiency, and B= annual mean biomass (µmolN/l).

Recently, several methods have been used to estimate the annual primary production (Annual PP) around Station P. The bold values in Table 3 are based on direct measurements and therefore are probably more accurate. Calculated values from NEMURO are given in Tables 4 and 5 using conversion factors from Table 6. A comparison of model output and diagnostics to field measurements can be summarized as follows:

1. The C/B and P/C ratios are reasonable (Tables 1 and 2).
2. The annual primary production in the model (128 gC/m^2/yr) is only 8% lower than the best current estimate (Table 3 - 140 gC/m^2/yr).
3. The average chlorophyll concentration at Station P in the model (Table 5 - 0.36 mg/m^3 is only 10% lower than the long-term value (0.4 mg/m^3) measured by Wong *et al.* (1995) (Table 7).
4. An approximate f-ratio can be estimated from the annual productivity of PL / Total primary production (Table 7). This estimate assumes that the production of the large phytoplankton (PL) is primarily fuelled by "new" nitrogen (NO_3) with "f-ratio"= 29.5/128 = 0.23. Wong *et al.* (1995) estimated an f-ratio of 0.25. So the agreement is good.

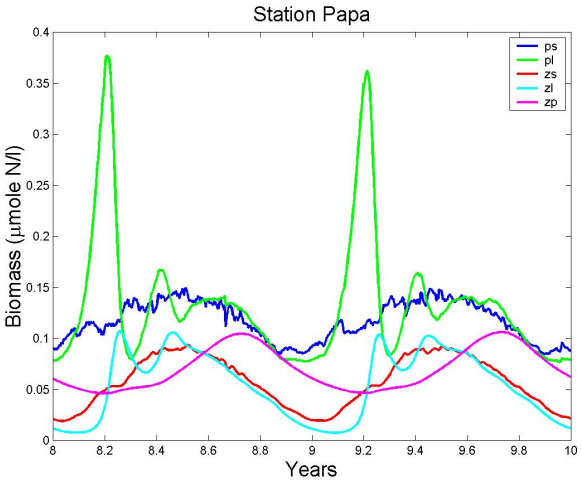

Fig. 4 NEMURO model base-case solution at Ocean Station Papa.

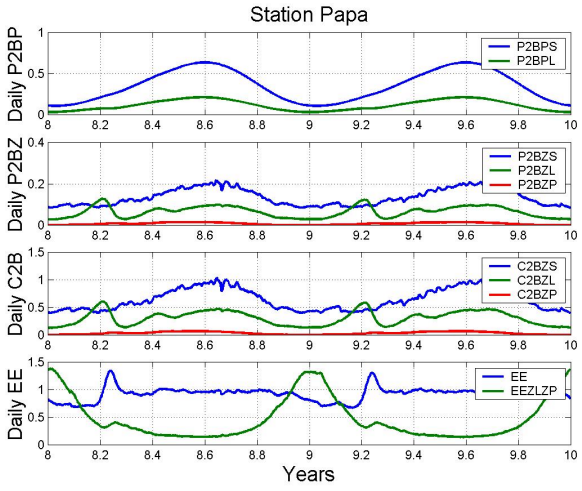

Fig. 5 P/B (production / biomass), C/B (consumption / biomass), P/C (production / consumption) ratios and Ecotrophic Efficiency.

Table 3 Estimates of Station P primary production.

Method	Average Daily PP ($gC/m^2/d$)	Annual PP ($gC/m^2/yr$)	Source
C14		**140**	Wong *et al.* 1995
Nitrate depletion		**133**	Wong *et al.* 1995
Particle flux		**120**	Wong *et al.* 1995
Chl *a*	0.55	199	Longhurst *et al.* 1995
Secchi disc data		167	Falkowski and Wilson 1992

Table 4 Average annual biomass (B1-B4), P/B, and annual primary production (PP) for PS and PL.

Group	B1 µmolN/l	B2 µmolC/l	B3 gC/m^3	B4 gC/m^2	P/B d^{-1}	PP $gC/m^2/yr$
PS	0.12	0.792	0.0095	0.760	0.355	98.5
PL	0.11	0.726	0.0087	0.697	0.116	29.5
PS + PL	0.23	1.518	0.0182	1.457		128

Calculations:

1. B2 = 6.6 (Redfield ratio) × B1
2. B3 = 0.012 × B2 (Table 6)
3. B4 = 80 m × B3 (Table 7)
4. PP = P/B × B4 × 365 d

Table 5 Average chlorophyll-*a* concentration of PS and PL.

Group	B3 gC/m^3	C/Chl *a*	Chl *a* mg/m^3
PS	0.0095	50	0.19
PL	0.0087	50	0.17
PS + PL	0.0182	50	0.36

Table 6 Conversion factors.

Variable	Value	Source
C/N (Redfield)	6.6	Wong *et al.* 1995
C/N	7.8	Kawamiya *et al.* 1997
N/Chl *a*	7.5	Kawamiya *et al.* 1997
C/Chl *a*	50	Kawamiya *et al.* 1997

Table 7 Station P Characteristics.

Variable	Value	Source
Euphotic zone	80 m	Wong *et al.* 1995
Average Chl *a* (annual)	0.4 mg/m^3 (µg/L)	Wong *et al.* 1995
f-ratio	0.25	Wong *et al.* 1995
f-ratio (summer)	0.25-0.52	Wong *et al.* 1998

Inclusion of microbial loop: sensitivity studies to climate change

Under certain scenarios, it is possible that changes in climate could lead to differences in the amount of primary production passing through the microbial loop. For example, an increase in stratification – due to increased freshwater inputs or higher temperatures – may reduce the nutrient entrainment to the euphotic zone, shifting the pelagic foodweb toward smaller species. We have modified the NEMURO/MATLAB Box model to include an approximation to a microbial loop as described in Megrey *et al.* (2000) and its possible effects on higher trophic levels. Using the same variable names as in Megrey *et al.* (2000), our simplified paramaterization of the microbial food web, which is included in the variable BetaZS is:

$$BetaZS = 0.3^{(1+\ PhySn/(PhySn+PhyLn))}$$

This means that the gross growth efficiency of the small zooplankton can vary between 0.3 and 0.09, and will probably average about 0.16 over the year at Station P. For the base model run, a constant BetaZS=0.3 was used. We found (Fig. 6) that the inclusion of a microbial loop has only a small impact on the standing stocks of small and large zooplankton, but reduces predatory zooplankton standing stocks by about one half. These differences are due to the decreased net trophic efficiency of the system when a large portion of the primary production passes through a microbial community before entering the zooplankton community. With the decreased predatory zooplankton biomass, there is only half as much biomass potentially available for fisheries production.

Vertical migration by large zooplankton: sensitivity studies

At Station P, during spring, the large zooplankton component (ZP) should be dominated by *Calanus/Neocalanus* spp. These species exhibit a strong ontogenetic migration: they arrive in the upper layers in early spring at C1 (and older) copepodites and feed for about 60 days until descending from the surface layer as C5's. Therefore, the model population should increase in

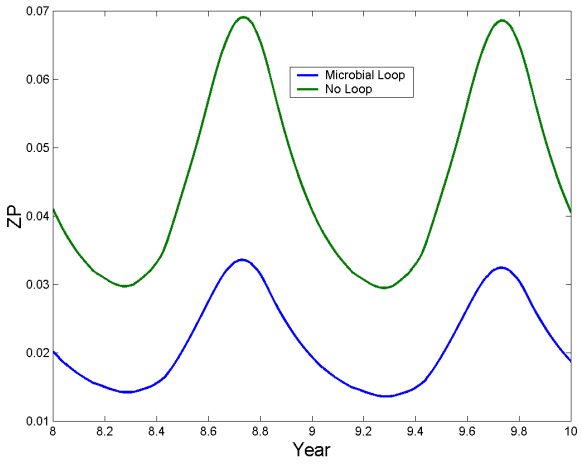

Fig. 6 Predatory zooplankton biomass (in µM N/m^3) for two years with (blue line) and without (green line) the inclusion of a microbial loop.

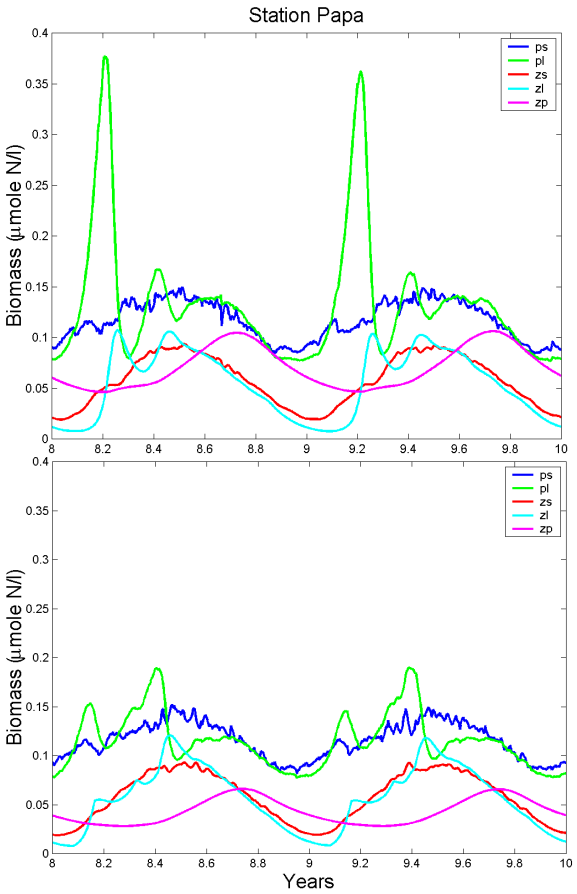

Fig. 7 Sensitivity at Station P to migration of large zooplankton (ZP). Without migration of ZP (top panel) the diatom bloom (PL) is close to twice as large as in the presence of ZP migration (bottom panel).

biomass in the early spring independent of food availability/grazing. Later in the year, the population should decrease by some amount to simulate the descent of the C5's. To explore this effect, we modified the model as follows. Over a certain time (between days-of-the-year 30 and 60), we increased the large zooplankton population five-fold. The increased population would be available to graze on the diatoms. Other dynamics occur as normal. After 60 more days, we begin decreasing the large zooplankton population by one half over 30 days (between days 120 and 150). Again, other dynamics are unchanged. Figure 7 shows results with and without migration. In the case of migration, the diatom (PL-large phytoplankton) bloom is much reduced. The estimates of Ecotropic Efficiency (not shown) are not significantly affected.

NEMURO Model follow up

Yasuhiro Yamanaka[1, 2]

[1] Graduate School of Environmental Earth Science, Hokkaido University, N10W5 Kita-Ku, Sapporo, Japan. 060-0810 E-mail: galapen@ees.hokudai.ac.jp

[2] Global Warming Research Program, Frontier Research System for Global Change, Shibaura 1-2-1, Minato-Ku, Tokyo, Japan. 105-6791

The model presented is based on the NEMURO / 1-D Yamanaka Model described in Megrey *et al.* (2000), but it is extended to 15 compartments including silica and carbon cycles. The extended model is applied to Station A7 offshore of Hokkaido Island (41°30' N, 145°30' E), in the northwestern Pacific, which is one of the stations along the A-line where the Hokkaido National Fisheries Research Institute has been conducting surveys 5-7 times each year from 1987 to 2000. The model successfully simulates the observed spring diatom blooms and large annual variation of chlorophyll-*a*. A comparison between cases with/without silicate limitation shows that the silicate limitation causes the decease of primary production by diatoms in the summer and the transition of phytoplankton species between diatoms and others.

Model description

The model and boundary conditions in this study are exactly the same as the NEMURO/1-D Yamanaka model or that in Kishi *et al.* (2001), except the original 11 compartments describing the biological processes where changed into 15. Figure 8 shows interactions among the 15 compartments in the biological processes. We divide phytoplankton and zooplankton into two categories, respectively: large phytoplankton (PL) and small phytoplankton (PS), large zooplankton (ZL) and small zooplankton (ZS). ZL represents copepods with seasonal vertical migration, i.e., coming up to upper layer in spring, becoming adults and grazing on other plankton, and then returning to the deep layer in fall. This treatment is similar to that in Kishi *et al.* (2001). ZS represents the others. PL is diatoms which make siliceous shells from silicate in the water. Therefore, the nutrient limitations for photosynthesis by PL are not only nitrogen but also silicate in the water, which are not taken into account in Kishi *et al.* (2001). PS represents the other phytoplankton, non-diatom and flagellate. Some of PS and ZS are regarded as coccolith and foraminifera, which have calcarious shells, respectively. Predatory zooplankton (ZP) represents something like euphausiids grazing on other plankton, which connect the lower trophic level food chain to the higher trophic levels such as fishes, following discussions at the PICES MODEL Workshop in Nemuro. The model also has three nutrients, nitrate (NO_3), ammonium (NH_4), and silicate ($Si(OH)_4$), particulate organic matter (POM), dissolved organic matter (DOM), Opal, calcium carbonate ($CaCO_3$). Calcium (Ca) in the sea water is taken into account, in order to calculate total alkalinity (TAlk) using the concentrations of NO_3, $Si(OH)_4$, Ca following the TAlk definition. Total carbon (TCO_2) is obtained with assumption that all plankton have the same C/N stoichiometry as classical Redfield ratio, 106/16.

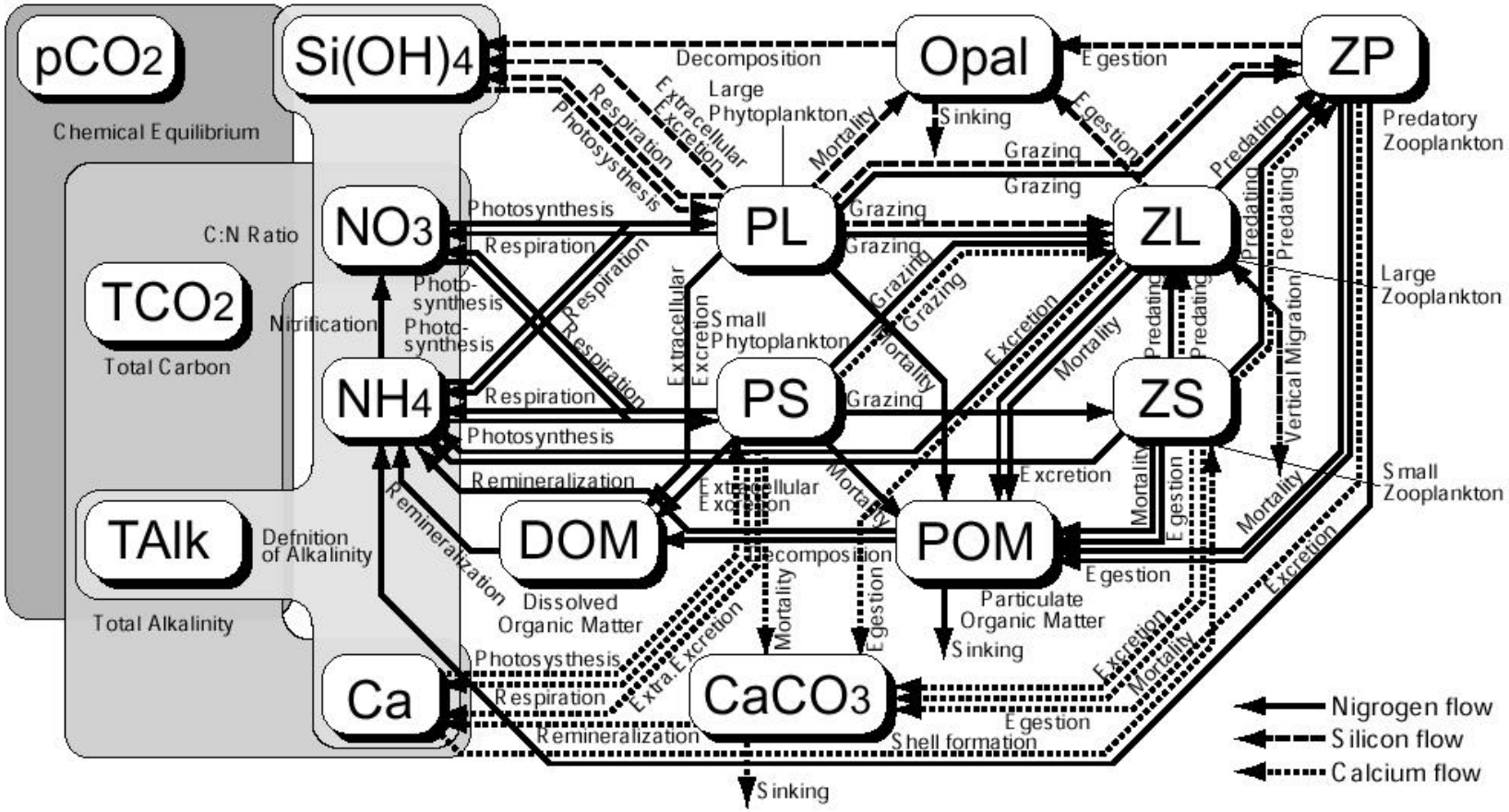

Fig. 8 Interactions among 15 compartments for a modification of the NEMURO/1-D Yamanaka Model.

Table 8 Biological parameters used in the model.

V_{maxS}	Small Phytoplankton Maxium Photosynthetic Rate at 0°C	0.4	/day
$K_{\mathrm{NO_3S}}$	Small Phytoplankton Half Saturation Constant for Nitrate	1.0	μmolN/l
$K_{\mathrm{NH_4S}}$	Small Phytoplankton Half Saturation Constant for Ammonium	0.1	μmolN/l
Ψ_{S}	Small Phytoplankton Ammonium Inhibition Coefficient	1.5	l/μmolN
k_{S}	Small Phytoplankton Temperature Coefficient for Photosynthetic Rate	0.0693	/°C
I_{optS}	Small Phytoplankton Optimum Light Intensity	104.7	W/m^2
M_{PS0}	Small Phytoplankton Mortality Rate at 0°C	0.0585	l/μmolN day
k_{MPS}	Small Phytoplankton Temperature Coefficient for Mortality	0.0693	/°C
R_{PS0}	Small Phytoplankton Respiration Rate at 0°C	0.03	/day
k_{RS}	Small Phytoplankton Temperature Coefficient for Respiration	0.0519	/°C
γ_{S}	Small Phytoplankton Ratio of Extracellular Excretion to Photosynthesis	0.135	(Nodim)
V_{maxL}	Large Phytoplankton Maxium Photosynthetic Rate at 0°C	0.8	/day
$K_{\mathrm{NO_3L}}$	Large Phytoplankton Half Saturation Constant for Nitrate	3.0	μmolN/l
$K_{\mathrm{NH_4L}}$	Large Phytoplankton Half Saturation Constant for Ammonium	0.3	μmolN/l
K_{SiL}	Large Phytoplankton Half Saturation Constant for Silicate	6.0	μmolSi/l
Ψ_{L}	Large Phytoplankton Ammonium Inhibition Coefficient	1.5	l/μmolN
k_{L}	Large Phytoplankton Temperature Coefficient for Photosynthetic Rate	0.0693	/°C
I_{optL}	Large Phytoplankton Optimum Light Intensity	104.7	W/m^2
M_{PL0}	Large Phytoplankton Mortality Rate at 0°C	0.029	l/μmolN day
k_{MPL}	Large Phytoplankton Temperature Coefficient for Mortality	0.0693	/°C
R_{PL0}	Large Phytoplankton Respiration Rate at 0°C	0.03	/day
k_{RL}	Large Phytoplankton Temperature Coefficient for Respiration	0.0519	/°C
γ_{L}	Large Phytoplankton Ratio of Extracellular Excretion to Photosynthesis	0.135	(Nodim)
G_{RmaxS}	Small Zooplankton Maxium Grazing Rate at 0°C	0.4	/day
k_{GS}	Small Zooplankton Temperature Coefficient for Grazing	0.0693	/°C
λ_{S}	Small Zooplankton Ivlev Constant	1.4	l/μmolN
$\mathrm{PS}^*_{\mathrm{ZS}}$	Small Zooplankton Threshold Value for Grazing Small Phytoplankton	0.043	μmolN/l
α_{ZS}	Small Zooplankton Assimilation Efficiency	0.7	(Nodim)
β_{ZS}	Small Zooplankton Growth Efficiency	0.3	(Nodim)
M_{ZS0}	Small Zooplankton Mortality Rate at 0°C	0.0585	l/μmolN day
k_{ZS}	Small Zooplankton Temperature Coefficient for Mortality	0.0693	/°C
$G_{\mathrm{RmaxL,PS}}$	Large Zooplankton Maxium Rate of Grazing Small Phytoplankton at 0°C	0.1	/day
$G_{\mathrm{RmaxL,PL}}$	Large Zooplankton Maxium Rate of Grazing Large Phytoplankton at 0°C	0.4	/day
$G_{\mathrm{RmaxL,ZS}}$	Large Zooplankton Maxium Rate of Predating Small Zooplankton at 0°C	0.4	/day
k_{GL}	Large Zooplankton Temperature Coefficient for Grazing	0.0693	/°C
λ_{L}	Large Zooplankton Ivlev Constant	1.4	l/μmolN
$\mathrm{PS}^*_{\mathrm{ZL}}$	Large Zooplankton Threshold Value for Grazing Small Phytoplankton	0.04	μmolN/l
$\mathrm{PL}^*_{\mathrm{ZL}}$	Large Zooplankton Threshold Value for Grazing Large Phytoplankton	0.04	μmolN/l
$\mathrm{ZS}^*_{\mathrm{ZL}}$	Large Zooplankton Threshold Value for Predating Small Zooplankton	0.04	μmolN/l
α_{ZL}	Large Zooplankton Assimilation Efficiency	0.7	(Nodim)
β_{ZL}	Large Zooplankton Growth Efficiency	0.3	(Nodim)
M_{ZL0}	Large Zooplankton Mortality Rate at 0°C	0.0585	l/μmolN day
k_{ZL}	Large Zooplankton Temperature Coefficient for Mortality	0.0693	/°C

Table 8 (*continued*)

$G_{\mathrm{RmaxP,PL}}$	Predatory Zooplankton Maxium Rate of Grazing Large Phytoplankton at 0°C	0.2	/day
$G_{\mathrm{RmaxP,ZS}}$	Predatory Zooplankton Maxium Rate of Predating Small Zooplankton at 0°C	0.2	/day
$G_{\mathrm{RmaxP,ZL}}$	Predatory Zooplankton Maxium Rate of Predating Large Zooplankton at 0°C	0.2	/day
k_{GP}	Predatory Zooplankton Temperature Coefficient for Grazing	0.0693	/°C
λ_{P}	Predatory Zooplankton Ivlev Constant	1.4	l/μmolN
$\mathrm{PL}^{*}_{\mathrm{ZP}}$	Predatory Zooplankton Threshold Value for Grazing Large Phytoplankton	0.04	μmolN/l
$\mathrm{ZS}^{*}_{\mathrm{ZP}}$	Predatory Zooplankton Threshold Value for Predating Small Zooplankton	0.04	μmolN/l
$\mathrm{ZL}^{*}_{\mathrm{ZP}}$	Predatory Zooplankton Threshold Value for Predating Large Zooplankton	0.04	μmolN/l
Ψ_{PL}	Predatory Zooplankton Preference Coefficient for Large Phytoplankton	4.605	l/μmolN
Ψ_{ZS}	Predatory Zooplankton Preference Coefficient for Small Zooplankton	3.010	l/μmolN
α_{ZP}	Predatory Zooplankton Assimilation Efficiency	0.7	(Nodim)
β_{ZP}	Predatory Zooplankton Growth Efficiency	0.3	(Nodim)
M_{ZP0}	Predatory Zooplankton Mortality Rate at 0°C	0.0585	l/μmolN day
k_{ZP}	Predatory Zooplankton Temperature Coefficient for Mortality	0.0693	/°C
α_1	Light Dissipation Coefficient of Sea Water	0.04	/m
α_2	Self Shading Coefficient	0.04	l/μmolN m
N_{Nit0}	Nitrification Rate at 0°C	0.03	/day
k_{Nit}	Temperature Coefficient for Nitrification	0.0693	/°C
S_{POM}	POM Sinking Velocity	40.0	m/day
V_{PA0}	Decomposition Rate of POM to Ammonium at 0°C	0.100	/day
k_{PA}	Temperature Coefficient for POM Decomposition to Ammonium	0.0693	/°C
V_{PD0}	Decomposition Rate of POM to DOM at 0°C	0.100	/day
k_{PD}	Temperature Coefficient for POM Decomposition to DOM	0.0693	/°C
V_{DA0}	Decomposition Rate of DOM at 0°C	0.200	/day
k_{DA}	Temperature Coefficient for DOM Decomposition	0.0693	/°C
S_{Opal}	Opal Sinking Velocity	40.0	m/day
V_{Opal}	Decomposition Rate of Opal at 0°C	0.100	/day
k_{Opal}	Temperature Coefficient for Opal Decomposition	0.0693	/°C
$S_{\mathrm{CaCO_3}}$	Calcium Carbonate Sinking Velocity	40.0	m/day
$V_{\mathrm{CaCO_3}}$	Decomposition Rate of Calcium Carbonate at 0°C	0.050	/day
$k_{\mathrm{CaCO_3}}$	Temperature Coefficient for Calcium Carbonate Decomposition	0.0693	/°C
R_{CN}	Stoichiometry of Carbon to Nitrogen	6.625	(Nodim)
R_{SiN}	Large Plankton Stoichiometry of Silicon to Nitrogen	2.0	(Nodim)
R_{coco}	Ratio of Cocolithophorids to Small Phytoplankton	0.1	(Nodim)
R_{fora}	Ratio of Foraminifera to Small Zooplankton	0.1	(Nodim)
R_{Cco}	Ratio of Inorganic Carbon to Total Carbon in Cocolithophorids	0.5	(Nodim)
R_{Cfo}	Ratio of Inorganic Carbon to Total Carbon in Foraminifera	0.5	(Nodim)

The 15 compartments described above, PL, PS, ZL, ZS, ZP, NO_3, NH_4, $Si(OH)_4$, POM, DOM, Opal, $CaCO_3$, Ca, TAlk, and TCO_2, are calculated as prognostic variables. The partial pressure of carbon dioxide (pCO_2) in the ocean surface is obtained from the TAlk and TCO_2 under the chemical equilibrium at each time step. The silica cycle coupled with the nitrogen cycle accounted for in the photosynthesis process by PL affects the ecosystem dynamics. On the other hand, carbon and calcium cycles do not affect ecosystem dynamics because carbon and calcium are plentiful in the water and do not limit primary production. Parameters used in this study are shown in Table 8. Most parameters are based on Kishi *et al.* (2001) and NEMURO, although some parameters, V_{maxL}, K_{NH4L}, K_{SiL}, V_{maxS}, and K_{NO3S}, are tuned to reproduce the observed data, as discussed in parameter studies (Yoshie *et al.* in preparation).

We use the coupled ecosystem model mentioned above with physical model, vertical one-dimensional model with mixed layer closure scheme, used in Kishi *et al.* (2001). Boundary conditions, SST, SSS, wind stress, solar radiation, are the same as described in Kishi *et al.* (2001). Time integration is performed for ten years using data of 1991, and after that actual forcing from 1991 to 1996.

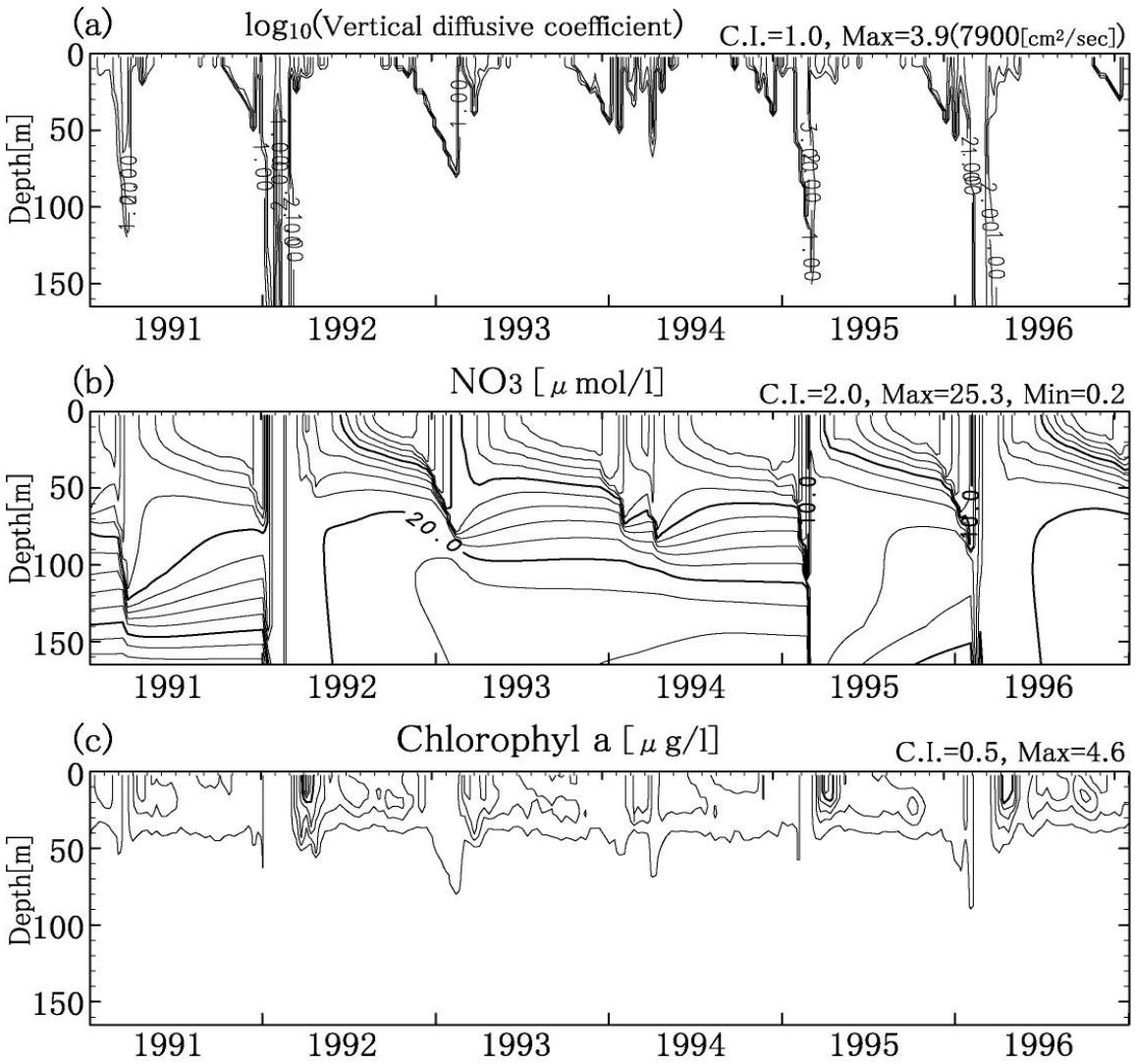

Fig. 9 Vertical distributions of (a) vertical diffusive coefficient, (b) nitrate concentration, and (c) chlorophyll-*a* concentration from 1991 to 1996.

Results

Figure 9 shows vertical distributions of vertical diffusive coefficient A_{HV}, nitrate concentration, and chlorophyll-*a* concentration from 1991 to 1996. Areas of high A_{HV} represent the mixed layer with seasonal changes. Deep convections in winter penetrated deeper than 160 m depths in 1992 and 1996. The nitrate-laden waters of almost 20 $x10^{-6}$ mol/l are supplied to the ocean surface associated with winter convections and cause a strong spring bloom by diatoms after winter. In 1992, the maximum value of chlorophyll-*a* concentration reaches $4.6x10^{-6}$ mol/l, which compares well with observed values during the spring bloom period. On the other hand, in 1993 or 1994, winter convections penetrated to around 70 m and the spring bloom was very weak. In summer, nutrients in the surface are exhausted and the maximum layer of chlorophyll-*a* concentration is located around 30 m. The model successfully reproduces the observed seasonal variations of nitrate, silicate, and chlorophyll-*a*, although the model cannot reproduce effects of horizontal advection/diffusion due to meso-scale eddy effects on nutrient and chlorophyll-*a* concentrations.

Figure 10a shows primary production by PL and PS and partial pressure of CO_2. The light solid line, primary production by diatoms, has highest

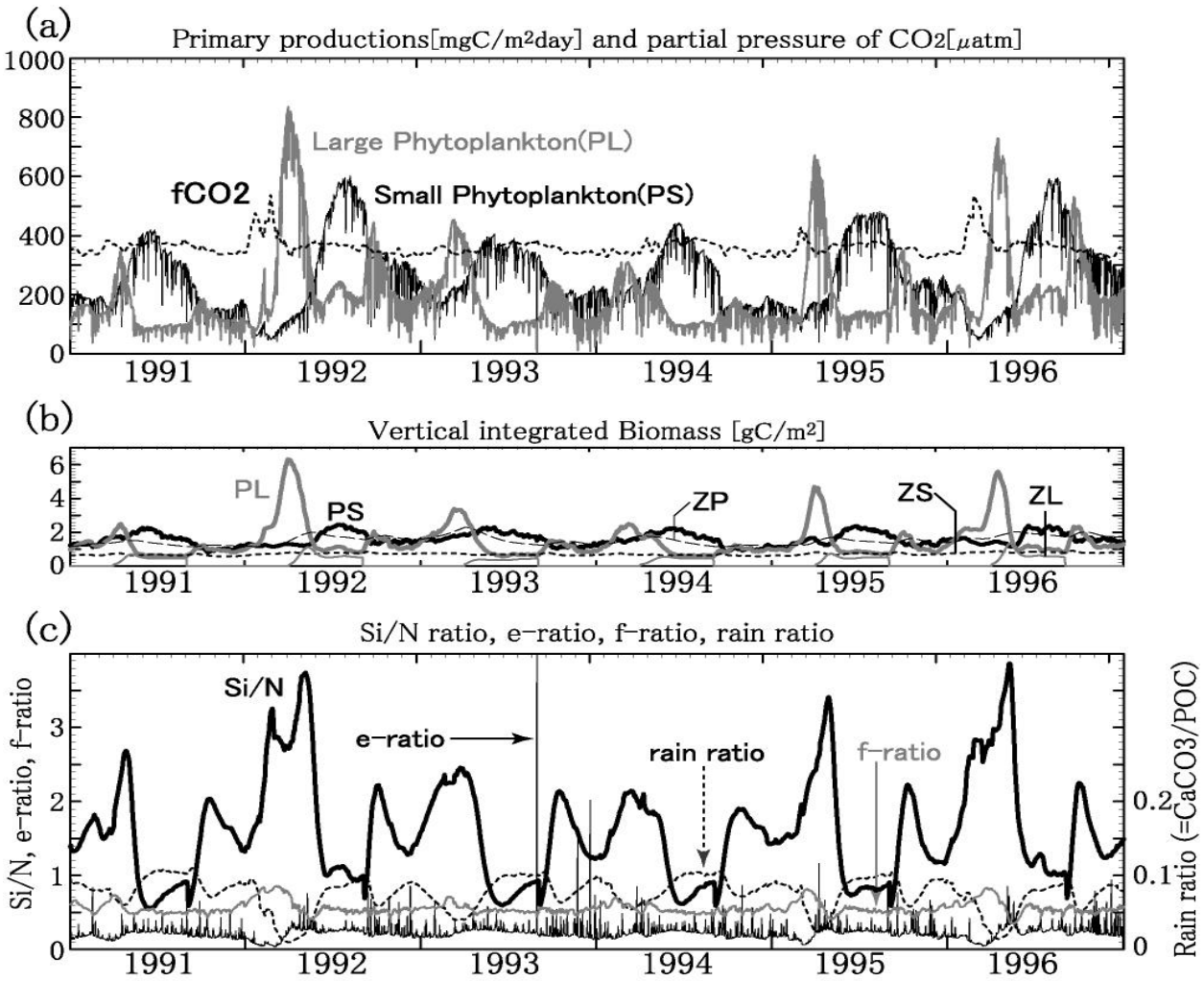

Fig. 10 Primary production by PL and PS, and partial pressure of CO_2 (a), vertically integrated biomasses of PS, PL, ZS, ZL, and ZP (b), and f-ratio, e-ratio, Si/N ratio, rain ratio (c) from 1991 to 1996.

peak in spring and the second highest peak in the fall. The spring bloom reaches 600 to 800 mg C/m^{2}day in 1992, 1995, and 1996, which compares well with observed levels. The spring bloom of diatoms has large annual variation, and the spring bloom in 1991 and 1994 is weak. The cessation of the spring bloom of diatoms is associated with increasing grazing pressure by copepods, although both nitrate and silicate in the surface water still remain over 10 x10^{-6} mol/l at the end of bloom. After the diatom bloom, primary production by PS increases, an often observed transition of species from diatoms to flagellates, and nitrate in the surface water is exhausted at the end of summer. Many frequent downward spikes of primary production's lines in Figure 10a can be seen. These represent decreases of primary production due to decreasing solar radiation on rainy or cloudy days. The partial pressure of carbon dioxide has a maximum associated with winter convection, rapidly decreases due to the spring bloom, and is kept almost constant, canceling out the temperature effect and biological production effect.

A dark thick line in Figure 10c shows Si/N ratio obtained from downward fluxes of opal and POM at depth of 100 m. The water supplied from the deep layer has a Si/N ratio of 1.7. Si/N ratios have large seasonal variations: about 3.0 in winter and spring, and about 1.0 in summer, although the total time average of the Si/N ratio in total settling particles is equal to 1.7. It looks inconsistent that a Si/N ratio of 3.0 is greater than the stoichiometry

of diatoms, i.e., Si/N ratio of 2.0. However, when copepods (ZL) and euphausiids (ZP) graze on diatoms, shells of diatoms are quickly discarded as settling opal and exported out of the euphotic layer. On the other hand, the soft tissue of diatoms become some of their bodies or DOM and nitrogen is recycled in the euphotic layer. Therefore, Si/N ratio takes a higher value than the stoichiometry of diatoms.

A light thin line in Figure 10c shows f-ratio, ratio of nitrate uptake to nitrogen uptake in the photosynthetic processes of PL and PS. The f-ratio is highest, 0.8, at the start of spring bloom, which is due to nitrate supply from the deep water associated with the winter deep convection, then decreases rapidly due to increase of ammonium and a decrease of nitrate as a result of the spring bloom, and takes a minimum of 0.3 (see f-ratio in 1996). In the other season, the f-ratio is kept almost constant at about 0.5. The e-ratio (a thin solid line), which is the ratio of downward flux due to POM to primary production, is smaller than 0.3, except for spikes due to small primary productions on bad weather days. The e-ratio is smaller by the factor of 2-3 than f-ratio, because POM is dissolved in the euphotic layer, and because organic matters directly returns to ammonium and nitrate by extracellular excretion and is quickly recycled. The rain ratio (a broken line in Fig. 10c), ratio of calcium carbonate flux to POC's at 100 m depths, is 0.01 to 0.11, which has the maximum in summer and minimum during the spring bloom.

A new approach to the modeling of marine ecosystems

Vladimir I. Zvalinsky
Pacific Oceanological Institute, 43 Baltiyskaya Street, Vladivostok, Russia. 690041 E-mail: biomar@mail.ru

The existing approaches to mathematical modeling of marine ecosystems are undergoing a crisis. This situation was evident to some extent in all reports concerning descriptions of the ecosystem function. At the MODEL Workshop in Nemuro this was also evident: it has left unsolved problems such as the limitation by additional environmental factors into the primary link (except light, nitrogen, and silicon), in particular, by Fe; as well as including the microbial link into the ecosystem. The problem of including higher trophic levels into the ecosystem has not been solved. The practical workers have proposed new questions such as splitting some trophic links into age groups, the behavior of which differs greatly.

The MODEL Task Team has done a lot of work. It has developed the Prototype Lower Trophic Level Ecosystem Model (NEMURO, Eslinger *et al.* 2000), which is a generalization of practically all of the most important developments on modeling marine ecosystems available in the published literature (Fasham *et al.* 1995; Kawamiya *et al.* 1997; Oguz *et al.* 1999). Due to this, the NEMURO model possesses both advantages and deficiencies typical of such models. That is why, in our opinion, the NEMURO model has significant difficulties in solving the problems described above.

The main problem in modern modeling of marine ecosystems is related to the fact that the approach to modeling is based on empirical models of each biological process, and, consequently, the ecosystem as a whole. The existing models do not involve the mechanisms of the biological processes.

From a strictly mathematical point of view, it is not important by which functions, empirical or those based on mechanism, to describe different processes. It is important that these functions reflect the real processes quite well. Still it is known that the empirical approaches are not only limited in application, but they do not make it possible to understand real processes, and, consequently, they do not possess the perspectives for the development of modeling.

The 20th century, especially the second half, is marked by the greatest discoveries in biophysics, biochemistry and physiology of organisms in general, and plants in particular. For example, in the field of primary production, being discovered were the carbon Calvin's cycle, two photosystems of photosynthesis, the water splitting system, photosynthetic and respiration electron-transport chains, cyclic and non-cyclic photo-phosphorylation, and photorespiration, (Edwards and Walker 1983; Goodwin and Mercer 1983). The peculiarities of carbon and nitrogen, phosphorus metabolism, and their interrelation were investigated; and the role of macro- and microelements in formation of primary production has been stated. An important achievement is establishing the fact that the biological processes present themselves as the chains and nets of coupling cyclic (in particular, enzymatic) interactions (Goodwin and Mercer 1983). These non-disputable facts are not presented in the most recent models of marine ecosystems.

The difficulties of analysis of mass fluxes for modeling of ecosystems are conditioned by non-homogeneity of the processes and structures forming the hierarchy of the ecosystem levels, starting from a cell up to the complicated assemblages of populations. With this, the necessity arises to couple the phenomena different in nature and temporal scales - physical-chemical ones, biochemical, physiological, and those of population. A unique approach to the description of such sort of systems is possible if the system is considered as the interaction of mass fluxes which is in accordance with the common laws of nature for the whole system.

Below an attempt is made to develop an approach to modeling marine ecosystems, starting from descriptions of separate biological processes and ending with the ecosystem as a whole.

Primary link of ecosystem

Primary production, i.e. the creation of organic matter, is central in the turnover of substances of the ecosystem. This link predetermines the volume of fluxes through all the other links. Understanding the processes of primary production and their adequate quantitative description is a determining one for the flow description in the ecosystem as a whole.

The processes of matter transformation into various trophic links of the ecosystem are based on general biochemical (enzymatic) mechanisms. Along with this, the primary production link differs from heterotrophic links, at least, in two ways: (1) the process rate depends on several substrate factors simultaneously, and (2) one of "substrates" of the process is the light energy. Matter flux through the heterotrophic link depends just on one substrate factor - food concentration, where the biogenous elements are relatively balanced.

Just these two circumstances create serious difficulties with quantitative modeling of the dependence of the primary production rate on the environmental factors which have not been coped with yet.

Photosynthesis scheme

Photosynthesis is the basis of primary production. A large number of generalized schemes of the process can be found in scientific literature (Edwards and Walker 1983; Goodwin and Mercer 1983). Figure 11 presents a simplified variant of "Z-scheme" of photosynthesis after Goodwin and Mercer (1983) in accordance with the modern notions. Even such a simplified scheme is a chain of 13 consecutive coupled cyclical reactions.

Two of them are cyclical transformations of oxidation-reduction of reaction centers PSII and PSI, coupled by an electron-transport chain consisting of five electron carriers. PSII receives an electron from water via a water-splitting system (Z) (cycle 1), and via an electron transport chain (cycles 3-7) transfers it to PSI. In its turn, PSI transfers an electron to acceptor (X), which via the carrier (cycle 10) reduces NADP to $NADH_2$ (cycle 11). $NADH_2$ is involved in poli-enzyme pentose-phosphate reduction cycle (Calvin's cycle), where CO_2 reduces to hydrocarbon (cycles 11-13).

An approach for the mathematical description of such kind of chains of cyclic coupled processes has been developed earlier (Zvalinsky and Litvin 1986). It has been shown that a linear chain of

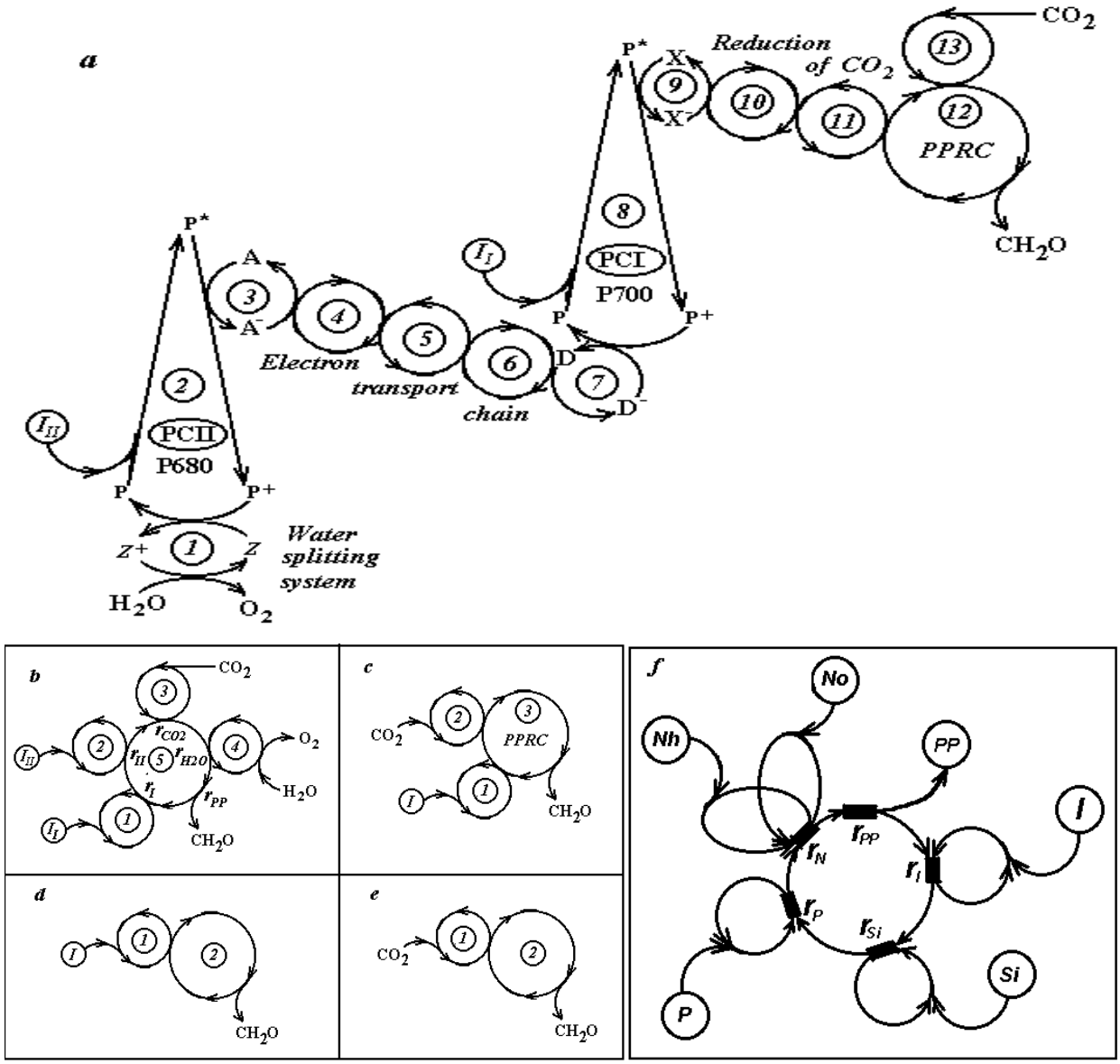

Fig. 11 Photosynthesis modeling by chains of coupling cyclical reactions of different complexity. (a) "Z-scheme" of photosynthesis – a chain of 13 consecutive coupling cyclical reactions; (b) a simplified model of photosynthesis for description of rate dependence on four substrates; (c) a simplified model for description of rate dependence on two substrates; (d) and (e) models for description of rate dependence on one substrate (light and CO_2); (f) a generalized model for description of primary production rate dependence on any number of substrates. For details see text.

coupled reactions is described by a linear chain fraction. For instance, for the scheme in Figure 11a, an equation for the description of the process rate with relation to the parameters of coupled reactions and values of the environmental factors - light intensity (I), CO_2 and H_2O substrate concentrations, will be as follows (to economize the space a fraction is divided into two parts):

Equation 1

$$\frac{r_{56}*V}{1-\frac{r_{45}*V}{1-\frac{r_{34}*V}{1-\frac{r_{23}*V}{1-\frac{V}{b*I_{II}}-\frac{r_{12}*V}{1-V/H_2O}}}}}+\frac{r_{67}*V}{1-\frac{r_{78}*V}{1-\frac{V}{a*I_I}-\frac{r_{89}*V}{1-\frac{r_{9,10}*V}{1-\frac{r_{10,11}'*V}{1-\frac{r_{11,12}'*V}{1-r_{PP}'*V-\frac{r_{12,13}*V}{1-V/CO_2}}}}}}}=1$$

Here: $V = P/P^m$ is the relative rate of the process with P and P^m as the rate and maximal rate of the process; $I_I = [I]/K_I$ and $I_{II} = [I]/K_{II}$ are the relative intensity of light in corresponding substrate constants PSI and PSII; α and β are the portions of the light absorbed by photo-systems I and II respectively; $H_2O = [H_2O]/K_{H2O}$ and $CO_2 = [CO_2]/K_{CO2}$ are the concentrations of water and carbon dioxide in the corresponding substrate constants; $K_{Si} = P^m/(k_{si}*[E_i^0])$ is a substrate constant with dimensions of concentration (k_{si} is a constant of incorporation rate of the i^{th} substrate; $[E_i^0]$ is the concentration of the component assimilating the i^{th} substrate); $r_{i,i+1} = P^m/\{k_{i,i+1}*[E_i^0]*[E_i+1^0]\} = P^m/P^m_{i,i+1}$ is a dimensionless generalized kinetic parameter marked as the 'resistance' of coupling reaction of the i^{th} and $i+1^{th}$ cycles and proportional to the time of the reaction progress ($k_{i,i+1}$ is a rate constant; E_i^0 and E_{i+1}^0 are total concentrations of reaction components; $P^m_{i,i+1} = k_{i,i+1}*[E_i^0]*[E_{i+1}^0]$ is the maximal rate of reaction of a corresponding link). The meaning of the $r_{i,i+1}$ parameter is analogous to that of diffusion 'resistance' or to the 'resistance' of carboxylation at photosynthesis (Edwards and Walker 1983). The inverse of resistance is the maximal relative link capacity or its conductivity

$$1/r_{i,i+1} = P^m_{i,i+1}/P^m.$$

We studied the kinetic characteristics of the chain fraction similar to Equation 1 (Zvalinsky and Litvin 1988a, b). The analysis has shown that if we do not consider oxidizing-reducing transformations of the components of the reaction chain, but just describe the dependence of the process rate on the substrates concentration, then the conceptual model and the corresponding mathematical model can be significantly simplified without considerable damage to the quality of the quantitative description. A five-cycle scheme presents a conceptual model of a four-substrate process (Fig. 11b). Mathematically, this model is described by:

Equation 2

$$\frac{r_I*V}{1-\frac{V}{a\times I}}+\frac{r_{II}*V}{1-\frac{V}{b\times I}}+\frac{r_{CO_2}*V}{1-\frac{V}{CO_2}}+\frac{r_{H_2O}*V}{1-\frac{V}{H_2O}}=1-r_{PP}*V$$

Here r_I, r_{II}, r_{CO2} and r_{H2O} are the relative coupling resistances of corresponding substrate cycles with the other reactions; r_{PP} is the total equivalent resistance of all cyclical reactions beyond the bounds of substrate cycles, and the rest are as in Equation 1. We see that in a simplified variant the dependence of rate on any substrate is described similarly, with no regard to its location in the chain of reactions (Fig. 11a): mathematically, the equation is relatively symmetric to any substrate (Eqn. 2).

In the case when the concentration of one of substrates is large ($H_2O \rightarrow \infty$, the value $[V/H_2O] \rightarrow 0$) and the limiting one is one of the photo-systems, the conceptual model of the process becomes three-cyclical (Fig. 11c), and Equation 2 becomes dependent on two factors:

Equation 3

$$\frac{r_I*V}{1-\frac{V}{a*I}}+\frac{r_c*V}{1-\frac{V}{CO_2}}=1-r_{PP}*V$$

Similarly, when one of two factors reaches saturation or is constant, the process model turns into a two-cycle one (Fig. 11d, e), and the dependence is reduced to a one-factor equation:

Equation 4

$$\frac{r_I * V}{1 - \frac{V}{a * I}} = 1 - r_{PP} * V$$

Equation 5

$$\frac{rc * V}{1 - \frac{V}{CO_2}} = 1 - r_{PP} * V$$

The relationships (4) and (5) are non-rectangular hyperbolas, the equations (2) and (3) are two-dimensional and four-dimensional non-rectangular hyperbolic surfaces correspondingly; and the equation (1) is the surface of higher order. The ratio between the kinetic parameters r_I can be found from the condition that at saturating values of concentrations, the process rate reaches its maximal value: at $I \rightarrow \infty$, $CO_2 \rightarrow \infty$ $P \rightarrow P^m$, $V \rightarrow 1$. For Equations 4 and 5, such condition is: $r_I + r_{PP} = 1$; $r_C + r_{PP} = 1$. Considering the above, Equations 4 and 5 can be rewritten in a more simple form:

Equation 6

$$[I] = K_I * \frac{V}{(1-V)} * (1 - r'_{PP} * V) \qquad \text{(a)}$$

$$[CO_2] = K_c * \frac{V}{(1-V)} * (1 - r''_{PP} * V) \qquad \text{(b)}$$

Dividing the first part of Equation 6a by V/(1 - V) gives a ratio important for the kinetics analysis:

Equation 7

$$[I] * \frac{1-V}{V} = K_I * (1 - r_{PP} * V)$$

It is seen from Equation 7 that in coordinates {[I]*(1 - V)/V} and V, that the whole hyperbolic family, rectangular and non-rectangular ones, possesses the form of a straight line with slope equal to $-r_{PP}$. With this, the continuation of the straight line cuts off the segment V_0 at the X-axis which is numerically equal to the reverse value of resistance $V_0 = 1/r_{PP}$, and at the Y-axis, the segment is equal to a substrate constant K_I (Fig. 12). The straight line parallel to the abscissa corresponds to the rectangular hyperbola of Michaelis-Menten. Analysis of experimental kinetic curves in these coordinates enables us to ascertain the character of dependence and to solve the problem of adequacy of the proposed models to the real biological processes. Moreover, such analysis allows to determine the values of parameters K_I and r_{PP} by modeling the process as a two-cyclical scheme (Fig. 11d-e, Fig. 12).

It is noteworthy that the maximal simplification of the reaction chain in Figure 11a is possible up to a one-substrate two-cyclic coupled reaction (Fig. 11e). In such 'minimal' two-cyclic model, the substrate incorporation and substrate processing take place in different systems of cyclical reactions. Further simplification up to one-cycle model is quite coarse and non-adequate, and it is possible in the only particular case when $r_{PP} \cong 0 << r_I \cong r_C \cong 1$, i.e. when ratios (Eqns. 4 and 5) pass into equations of rectangular hyperbola of Michaelis-Menten for the one-cyclical one-enzymatic reaction.

Comparison to the experiment

We have carried out a great number of experiments to measure the light and CO_2 dependence of the rate of marine alga photosynthesis. The data testify that the real dependencies are described by the equation of non-rectangular hyperbola (4) and (5) with a sufficiently high accuracy (Zvalinsky and Litvin 1988a, 1988b). The values $r_{PP} \cong 0.95$, and $r_I \cong r_C \cong 0.05$ have been determined experimentally both for the light and CO_2 curves of photosynthesis. Non-rectangular hyperbola with such parameters is the most similar to the hyperbolic tangent (Platt *et al.* 1977). It means that the rate of substrate incorporation (may) as a rule exceed the rate of substrate processing by not less than ~20 times. Also, the tests have shown high accuracy in describing photosynthesis rate by Equation 3 using two factors at a time (light intensity and CO_2 concentration, Fig. 12).

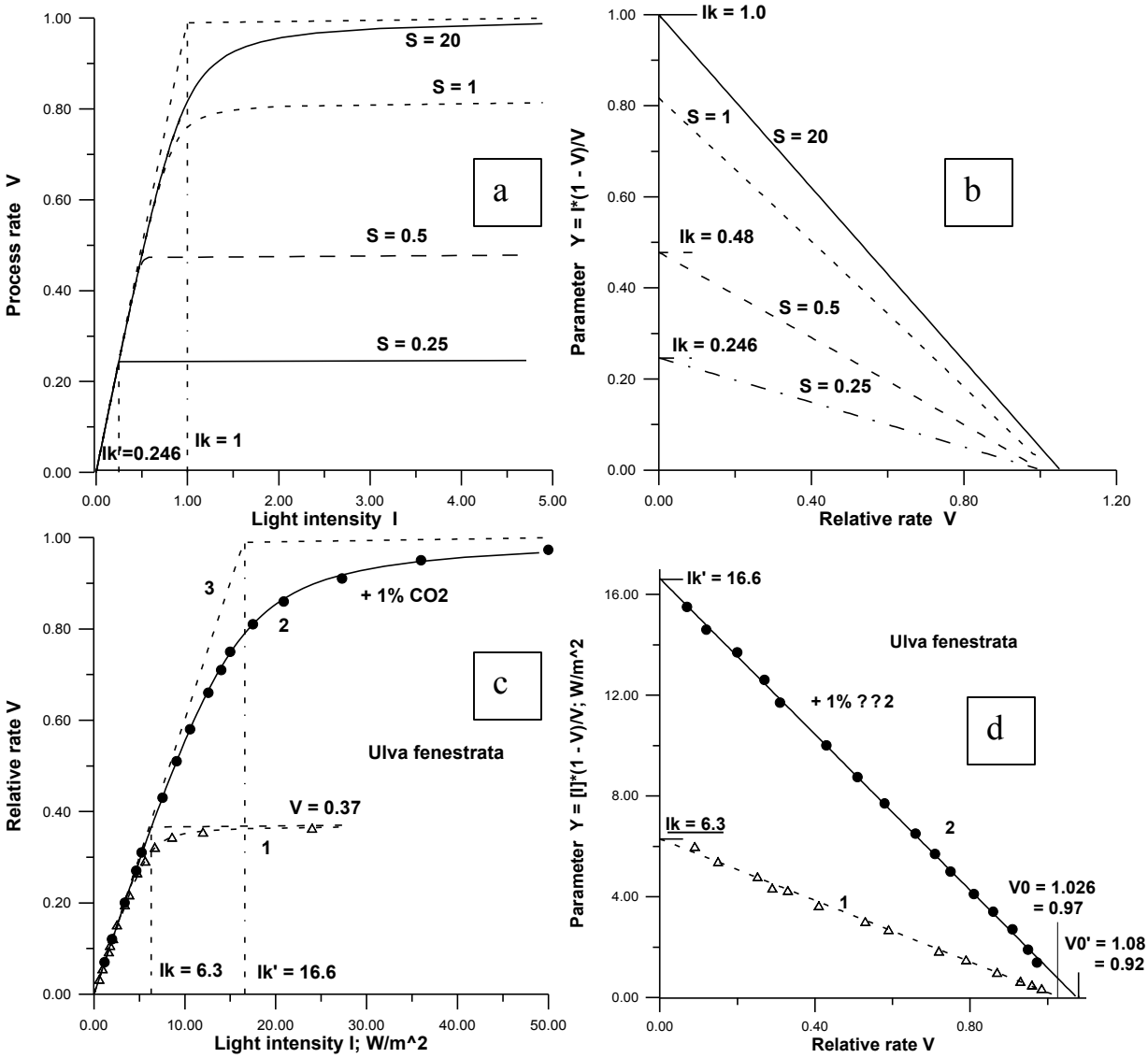

Fig. 12 The comparison of theoretical and experimental dependencies of process rate on two substrates in usual (a, c) and special (I*(1-V)/V against V, band d) coordinates. (a) the two-substrate (I - S) model as a chain of three coupled cyclical (enzymatic) reactions, the light-saturation curves are given for the different levels of other substrate 'S'; (b) the same curves in special coordinates; (c) the experimental dependence of seaweed photosynthesis on light in seawater (1), and in seawater saturated by air with 1% of CO_2 (2); (d) the same curves in special coordinates. The experimental dependencies are in a good agreement with the theoretical non-rectangular hyperbola.

Michaelis-Menten equation or non-rectangular hyperbola

In the NEMURO model, the dependence of the primary production rate on the concentration of nutrients is described by equations of rectangular hyperbola (Eqns. 1 and 2 in Eslinger *et al.* 2000). As it was noted above, all substrates are incorporated into the reaction chain via the corresponding enzymes (components, Fig. 11a) in the same manner, so conceptually and mathematically the process dependence on substrates should be described by a similar type of functions, non-rectangular hyperbola (Eqns. 2 and 5). Usage of Michaelis-Menten equation is not correct and can lead to quite low accuracy and non-adequacy of the description.

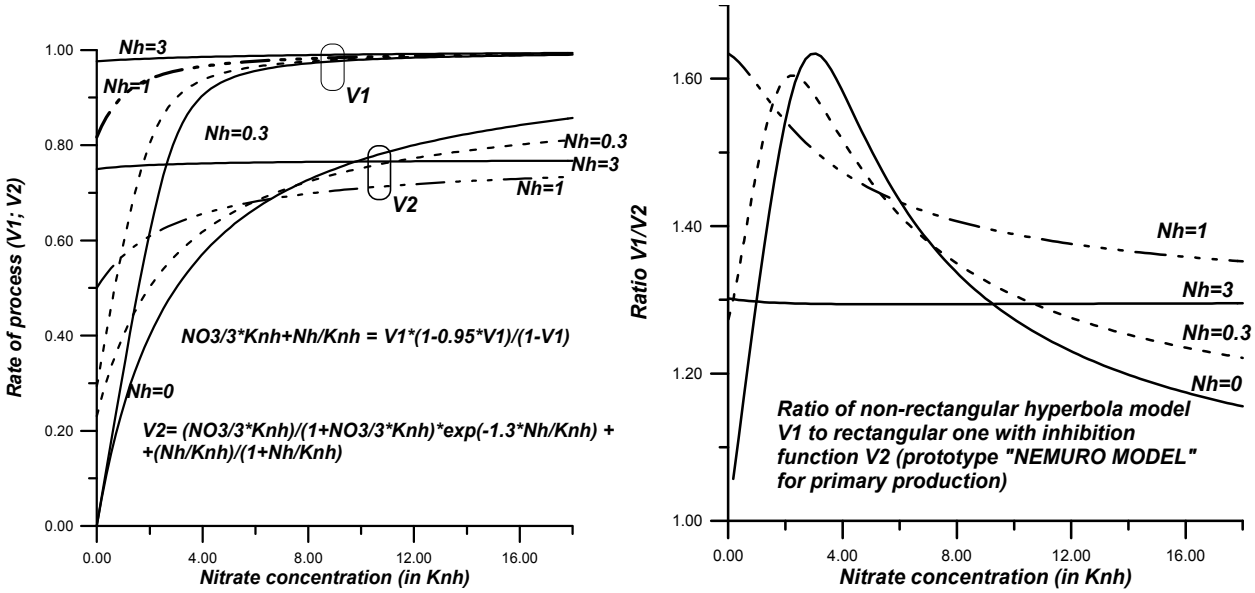

Fig. 13 Left panel: A comparison of non-rectangular hyperbola PP model with two competition substrate (nitrate and ammonium) V_1 with the NEMURO Model prototype V_2. Right panel: The ratio of these two type curves. The PP dependence curves on one of substrates (nitrate) are presented for different values of other (ammonium: Nh = 0.0; 0.3; 1.0 and 3.0 K_{nh}). The NEMURO Model results 1.2 – 1.6 times lower than non-rectangular model ones.

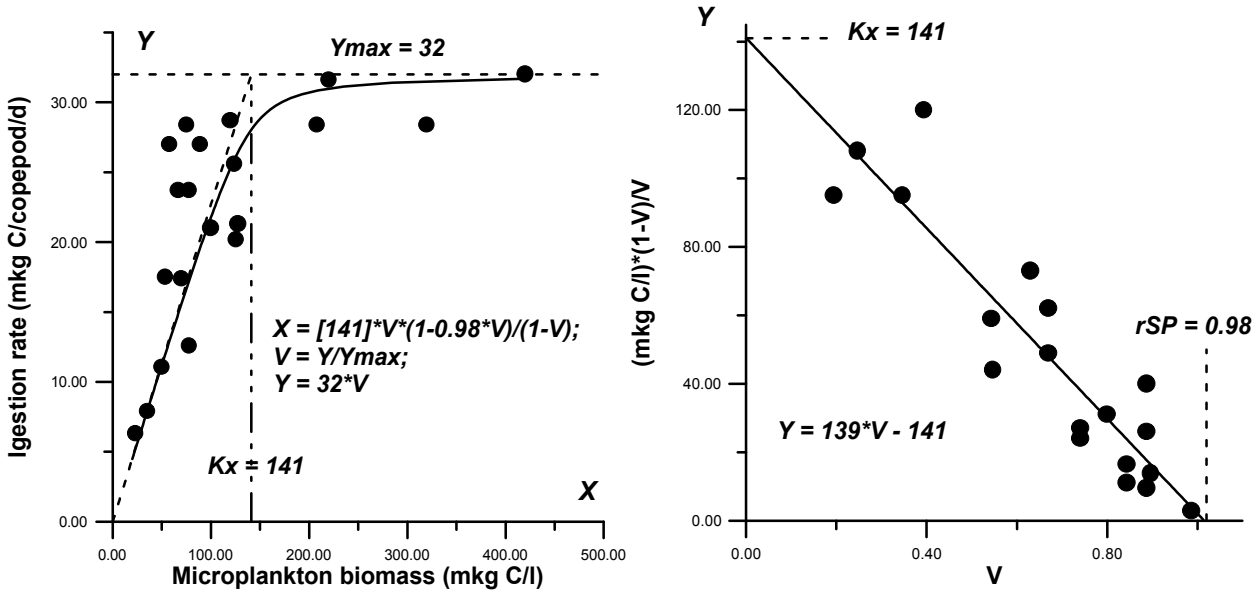

Fig. 14 Left panel: The ingestion rate of *Calanus sinicus* in relation to microplankton food supply (circles) using a theoretical curve of non-rectangular hyperbola with parameters found from data in the right panel. It is seen that K_X is not equal to substrate concentration, where rate Y = Ymax/2. Right panel: The same experimental points in linear space; Experimental points from Shiotani and Uye (2000). The regression equation and parameters of non-rectangular hyperbola are as follows: rSP = 0.98; substrate constant K_X = 141).

Inhibition or preference?

In the NEMURO model the competitive ratios of ammonium nitrogen and nitrate nitrogen consumption and also the grazing rates of large-phytoplankton and small-zooplankton to predator-zooplankton are described by introducing the inhibition function (Eqns. 1-2 and 13-14 in Eslinger *et al.* 2000). With this, inhibition takes place at quite a low concentration of substrate (food) comparable to the value of the Michaelis constant. Still, in physiology it is considered that inhibition takes place only at the highest values of substrate concentrations (many times exceeding the Michaelis constant, Edwards and Walker 1983). At low values, it is more expedient to speak not about the inhibition, but about the 'preference'. So, for two forms of nitrogen the equation of non-rectangular hyperbola (4) looks like:

Equation 8

$$\frac{r_N * V}{1 - V/(N_1 + N_2)} = 1 - r_{PP} * V$$

Concentrations of nitrogen and ammonium are expressed in the corresponding substrate constants $N_1 = [NO_3^-]/K_1$ and $N_2 = [NH_4^+]/K_2$.

Analysis has shown that the equation with inhibition (Eqns. 1-2 in Eslinger *et al.* 2000) gives values that are significantly lower than those calculated from to the equation of non-rectangular hyperbola with the light preference (Eqn. 8, Fig. 13). This distinction is especially high in the region of low and moderate concentrations (up to 60%), which is the most widespread situation in nature. As far as the tests confirm the adequacy of description of kinetics of the production process by the equation of non-rectangular hyperbola, the usage of Equation 8 with 'preference', from our point of view, should describe the process with higher precision than the function with inhibition.

General model of primary production

By analogy with the scheme of photosynthesis (Fig. 11a), a conceptual model of primary production of any complexity, incorporating any quantity of substrates (light, nutrients) can be made. The model can be maximally simplified with the aim of describing the primary production rate in relation to the environmental factors. For four factors - light intensity and concentration of main nutrients (two forms of nitrogen, phosphorus, and silicon) the model is given in Figure 11f.

The production rate *P* will be described by a system of two equations:

Equation 9

$$P = P^m * V$$

$$\frac{r_I * V}{1 - V/I} + \frac{r_N * V}{1 - V/(N_1 + N_2)} + \frac{r_P * V}{1 - V/P} + \frac{r_S * V}{1 - V/S} = 1 - r_{PP} * V$$

Here, the environmental factors are expressed in units of substrate constants: light intensity -$I = [I]/I_k$; concentration of nitrogen and ammonium - $N_1 = [NO_3^-]/K_1$ and $N_2 = [NH_4^+]/K_2$; phosphates - $P = [PO_4^{3+}]/K_P$; silicates -$S = [Si_{O3}^{2+}]/K_S$. The relative rate is $V = P/P^m$. Parameters r_I, r_N, r_P and r_S - relative coupling resistance of corresponding substrate cyclical process with the extra-substrate cyclic processes; parameter r_{PP} is the relative resistance of an assemblage of the extra-substrate reactions.

If the factor is not limiting (for instance, silicates; $S \to \infty$, $V/S \to 0$), then the denominator of the corresponding term (Eqn. 9) turns into 1.0 and this term can be incorporated into the last member of the right part. Equation 9 is transformed into a three-substrate one with $r_{PP}' = (r_{PP} + r_S)$. Similarly, it can be simplified until the level of two- and one-substrate equation (Eqns. 3 and 4). One of the terms of Equation 9 can be replaced by the other one, or a term can be included with the other limiting factor (for example, CO_2 or iron).

Thus, a system of equations (Eqn. 9) involves practically all possible variants of models for the primary production rate. This model, in our opinion, possesses a series of advantages compared to models published elsewher, as well as to NEMURO (Eqns. 1-2 in Eslinger *et al.* 2000). First of all, and this is the most important thing, the model has been developed on the basis of modern notions of the mechanism of the primary

production process. It includes parameters with clear biological meaning, and has quite a simple mathematical presentation. The model adequately describes the interrelationship of the factors, including competitive ones, the change of limitation from one factor to another without any additional conditions. The model can be naturally simplified or extended, with regard to the needs of the experiment or new knowledge (for instance, incorporation of limitation by iron or some other elements). It is naturally incorporated into the ecosystem model.

Photo-inhibition and photo-adaptation

The NEMURO model considers that the rate of primary production is inhibited by high light intensity (Steele 1962; Eqns. 1-2 in Eslinger *et al.* 2000). In plant physiology, it is usually assumed that instant light-saturation curves are measured in such a way that during the period of measurements the parameters of the production system do not change (i.e., when the processes of the light adaptation or inhibition do not manifest themselves). Just for this case, the model of primary production has been obtained. If a plant cell is in the light for a long time then the cell changes its parameters according to this light intensity, and an adaptation takes place. Our approach considers this process and allows a light curve of any form (Zvalinsky and Litvin 1991).

Heterotrophic links

Microbial link

Incorporation and metabolism of organic and mineral matters in a microbial cell is analogous to similar processes in a plant cell. That is why our one-, two-, and more-substrate models (Eqns. 1-9) can also be used to describe even bacterial cell growth rates.

Heterotrophic links of LTL

Grazing is also a chain of coupled cyclical processes: periodic food capture and the stomach filling in with its subsequent clearing due to the polyenzymatic food processing (Fasham 1995). Food processing needs one more substrate - oxygen. Consequently, in the simplest case grazing can be presented by a two-substrate (food and oxygen) three-cycle model (Fig. 11c, Eqn. 3) or as a one-substrate two-cycle model with the dependence on food concentration (the process is not limited by oxygen) (Fig. 11e, Eqn. 6b).

The grazing rate *G* for any trophic level and for any number of food types *Fn* with different preferences can be described by non-rectangular hyperbola:

Equation 10

$$\frac{r_G * V}{1 - V/(F_1 + F_2 + \ldots + F_n)} = 1 - r_{HP} * V;\ G = G^m * V$$

Here: G and G^m are the grazing rate and maximum grazing rate; V is the relative grazing rate; $F_1 = [F_1]/K_1$; $F_2 = [F_2]/K_2$; …, $F_n = [S_n]/K_n$ are the food concentrations in units of their substrate constants; ($[F_1]$, $[F_2]$, …, $[F_n]$ are concentrations of different food types, with K_1, K_2, …, K_n as their substrate constants). The substrate constants reflect the 'preference' factor. Values of r_G and r_{HP} are the parameters of the non-rectangular hyperbola. Values of r_G and r_{HP} reflect the resistances of capture and processing, respectively. The analysis of experimental data show that the ingestion rate of *Calanus sinicus* in relation to microplankton food supply describes well by Equation 10 with $r_{HP} = 0.98$ and $r_G = 0.02$ (Fig. 14).

As the rate of food capture exceeds by many times the rate of its processing, then, as in case of primary production $r_{HP} >> r_G$ ($r_G \approx 0.02$ - 0.05 and $r_{HP} \approx 0.95 - 0.98$). Non-rectangular hyperbola with such parameters is very similar to the hyperbolic tangent, i.e. it has longer initial segment and reaches the saturation sooner as compared to the exponent (Platt *et al.* 1977). As with the case of several forms of nitrogen, using the current grazing function in NEMURO to describe grazing in the presence of several kinds of food is not sufficiently grounded (Eqns. 13-14 in Eslinger *et al.* 2000). It is difficult to imagine a mechanism of such 'inhibition', especially, if we take into account that it persists at low food concentration. Non-rectangular hyperbola (Eqn. 10) with different 'preference' to different kinds of food is closer to the real processes.

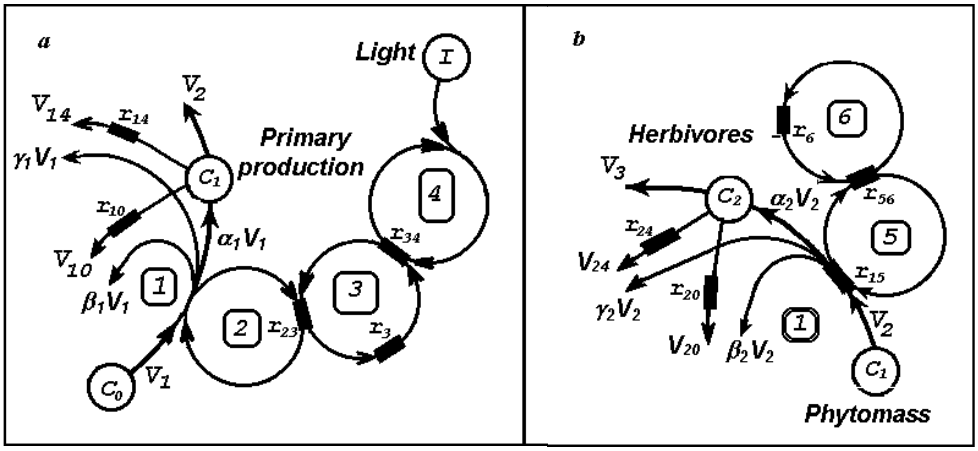

Fig. 15 The conceptual models of two-substrate primary production (a), and unisubstrate secondary production (b), with input and output (spending) fluxes of matter. Input fluxes: V_1 – incorporation of inorganic matter C_0 and V_2 – grazing rate of phytomass to herbivore (α_1 and α_2 – ecotrophic coefficients). Output fluxes: β_1V_1 and β_2V_2 – biosynthesis respiration; γ_1V_1 and γ_2V_2 – excretion and egestion; V_{10} and V_{20} – maintenance respiration expenses of C_1 or C_2; V_{14} and V_{24} – mortality; V_2 and V_3 – grazing phytoplankton and zooplankton to next trophic links.

Higher trophic levels

Grazing in the HTL and LTL do not differ considerably. HTL animals must first capture then process the food (polycyclical polyenzymatic food processing). Dependence of the HTL grazing rate in relation to the food supply can be described by the same function as for the LTL (Eqn. 10).

Inputs and outputs of different trophic links

The models described above refer to the input fluxes of different trophic links. Besides the input fluxes there are several output fluxes in each link. Figure 15a presents a primary link with 1 input flux (incorporating inorganic matter C_0 in the primary link) and 5 types of output fluxes: biosynthesis respiration, excretion, maintenance respiration expenses of phytoplankton biomass c_1, mortality, and phytoplankton grazing to the next trophic link.

Figure 15b presents fluxes for the secondary link - an input flux (grazing rate of phytomass to herbivore) and 5 output fluxes: biosynthesis respiration, egestion, maintenance respiration expenses of herbivore biomass c_2, mortality, and herbivorous zooplankton grazing to next trophic link. Unlike in the NEMURO model, respiration in each line is divided into two parts - biosynthesis respiration and maintenance respiration. They differ in the following. Biosynthesis respiration occurs at the expense of the eaten food and is proportional to the biomass of this food, when there is no food, this type of respiration is absent. Maintenance respiration takes place at the expense of the individual's biomass and does not depend on the volume of food eaten. This type of respiration predetermines the threshold of an organism's existence: if the volume of food eaten does not compensate the expenses of maintenance respiration, the organism dies (Edwards and Walker 1983). Just the maintenance respiration of the phytoplankton predetermines the boundary of the photic layer.

Ecosystem modeling

Conceptual model of any complicity ecosystem can be constructed by the consecutive and parallel linking of its different compartments (Fig. 15) with each other in accordance with direction of matter flows.

Figure 16 presents one version of this type of model consisting of six compartments. Four of these compartments are the biological ones (primary link, herbivores, carnivores and bacteria)

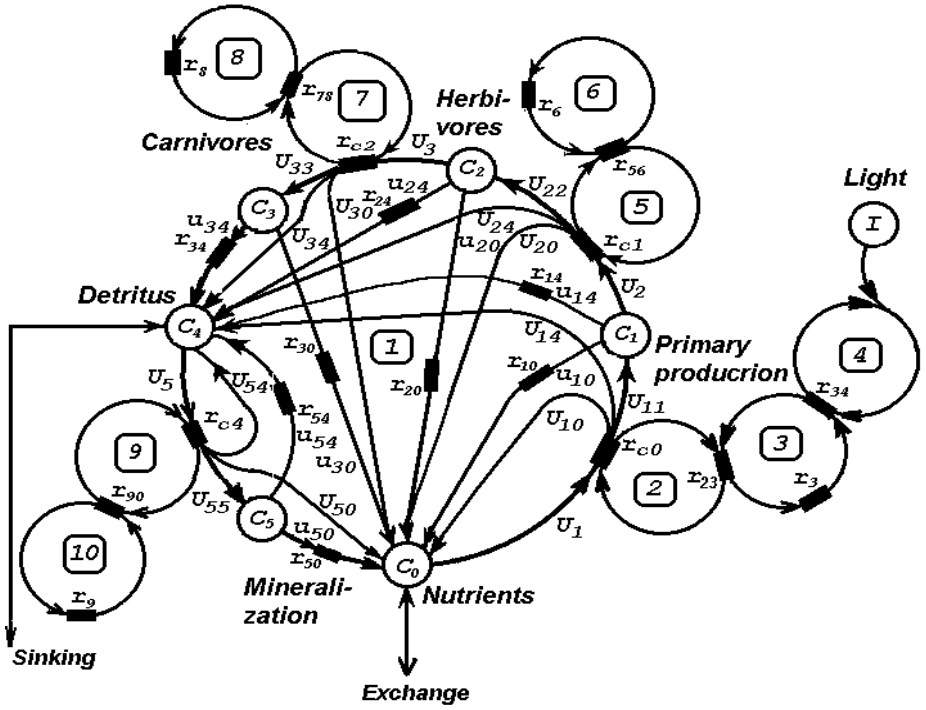

Fig. 16 The conceptual model of six-compartment ecosystem. The masses Ci of different trophic levels are drawn by circles. The arrows show the direction of matter flow between compartments. The kinetic parameters r_{ij} reflect types of interactions and determine the value of fluxes. For explanation and designation see the relevant sections in the text and in the Tables.

and two of them are non-living compartments (nutrients and detritus). All ecosystem fluxes of matter are closed. All fluxes and kinetic parameters are expressed in terms of main primary production flow P_1^m, all matter concentrations – in terms of total ecosystem concentrations of corresponding elements. Such ecosystem presentation is very convenient because it gives the possibility to write the equation system similar to graph method. This model is described by a system of 26 algebraic and differential equations (Tables 9 and 11). The parameters of the first three links are close to parameters of "average phytoplankton", "average herbivorous zooplankton" and "average carnivorous zooplankton" of NEMURO model (Eslinger *et al.* 2000). It is seen that the value of total resistance of link is inversely related to its maximum grazing (uptake) rate.

Figure 17 shows the time-dependence dynamics of ecosystem component concentrations that were calculated using equations of Table 9 and parameters of Table 11. The calculations were carried out using a specially developed program in TURBO PASCAL 7. The comparison of Figure 17a-f shows high sensitivity to changes of parameters. So, a relatively small increase of carnivore biomass spending (from 7% to 16% of maximum grazing) leads to a chain of changes: noticeable decreasing its own biomass, increasing of biomass of previous link and decreasing of primary link (compare Fig. 17a, b). The drastic shifts in biomasses are observed when the substrate constants (the analogue of half-saturation constants) change (compare Fig. 17b with c and d). The great decrease in herbivore substrate constant leads to drastic decreases in primary link biomass. The bulk of total mass exists in non-living forms (detritus and inorganic matter; compare Fig. 17d and e). There is revealed the tendency toward oscillations in this case. Using the Michaelis-Menten rectangular hyperbola for nutrient uptake instead of the non-rectangular hyperbola, is equivalent to decreasing the substrate constant which leads to corresponding declines in the primary link biomass (Fig. 17f). The tendency toward oscillations increases.

Table 9 Simultaneous equations for description of a six-compartment ecosystem.

No.	Equations for specific fluxes and mass compartment balance	Equations for full fluxes	Notes
	1. Primary production		
1.1.	$C_0 = \dfrac{r_{c0} * V_1}{1 - \dfrac{r_{23} * V_1}{1 - r_3 * V_1 - \dfrac{r_{34} * V_1}{1 - V_1 / I}}}$	$U_1 = C_1 * V_1$ $U_{11} = \alpha_1 * C_1 * V_1$	Incorporation of nutrients Phytomass accumulation
1.2.	$V_{10} = \beta_1 * V_1$	$U_{10} = \beta_1 * C_1 * V_1$	Biosynthesis respiration
1.3.	$v_{10} = 1/r_{10}$	$u_{10} = C_1 * v_{10}$	Maintenance respiration at the expense of c_1-biomass
1.4.	$V_{14} = \gamma_1 * V_1$	$U_{14} = \gamma_1 * C_1 * V_1$	Excretion
1.5.	$v_{14} = 1/r_{14}$	$u_{14} = C_1 * v_{14}$	Mortality
1.6.	$dC_1/dt = U_{11} - (u_{10} + u_{14} + U_2)$		Balance of c_1 biomass
	2. Herbivore link		
2.1.	$C_1 = \dfrac{r_{c1} * V_2}{1 - \dfrac{r_{56} * V_2}{1 - r_6 * V_2}}$	$U_2 = C_2 * V_2$ $U_{22} = \alpha_2 * C_2 * V_2$	Grazing rate of phytomass to herbivore Accumulation of c_2-biomass
2.2.	$V_{20} = \beta_2 * V_2$	$U_{20} = \beta_2 * C_2 * V_2$	Biosynthesis respiration
2.3.	$v_{20} = 1/r_{20}$	$u_{20} = C_2 * v_{20}$	Maintenance respiration at the expense of c_2-biomass
2.4.	$V_{24} = \gamma_2 * V_2$	$U_{24} = \gamma_2 * C_2 * V_2$	Excretion (egestion)
2.5.	$v_{24} = 1/r_{24}$	$u_{24} = C_2 * v_{24}$	Mortality
2.6.	$dC_2/dt = U_{22} - (u_{20} + u_{24} + U_3)$		Balance of c_2 biomass
	3. Carnivore link		
3.1.	$C_2 = \dfrac{r_{c2} * V_3}{1 - \dfrac{r_{78} * V_3}{1 - r_8 * V_3}}$	$U_3 = C_3 * V_{3+}$ $U_{33} = \alpha_3 * C_3 * V_3$	Grazing rate herbivore to carnivore Accumulation of c_3-biomass
3.2.	$V_{30} = \beta_3 * V_3$	$U_{30} = \beta_3 * C_3 * V_3$	Biosynthesis respiration
3.3.	$v_{30} = 1/r_{30}$	$u_{30} = C_3 * v_{30}$	Maintenance respiration at the expense of c_3-biomass
3.4.	$V_{34} = \gamma_3 * V_3$	$U_{34} = \gamma_3 * C_3 * V_3$	Excretion (egestion)
3.5.	$v_{34} = 1/r_{34}$	$u_{34} = C_3 * v_{34}$	Mortality
3.6.	$dC_3/dt = U_{33} - (u_{30} + u_{34})$		Balance of c_3 biomass
	4. Bacterial link		
4.1.	$C_4 = \dfrac{r_{19} * V_5}{1 - \dfrac{r_{90} * V_5}{1 - r_9 * V_5}}$	$U_5 = C_5 * V_5$ $U_{55} = \alpha_5 * C_5 * V_5$	Utilization rate detritus to bacteria Accumulation of c_5-biomass
4.2.	$V_{50} = \beta_5 * V_5$	$U_{50} = \beta_5 * C_5 * V_5$	Biosynthesis respiration
4.3.	$V_{50} = 1/r_{50}$	$u_{50} = C_5 * v_{50}$	Maintenance respiration at the expense of c_5-biomass
4.4.	$V_{54} = \gamma_5 * V_5$	$U_{54} = \gamma_5 * C_5 * V_5$	Excretion
4.5.	$V_{54} = 1/r_{54}$	$u_{54} = C_5 * v_{54}$	Mortality
4.6.	$dC_5/dt = U_{55} - (u_{50} + u_{54})$		Balance of c_5 biomass

Table 9 (*continued*)

	5. Equations of continuity	***Notes***
5.1.	$dC_4/dt = (U_{14} + u_{14} + U_{24} + u_{24} + U_{34} + + u_{34} + U_{54} + u_{54}) — U_5$	Balance of c_4 biomass
5.2.	$C_0 = 1 — (C_1 + C_2 + C_3 + C_4 + C_5)$	Balance of c_0 biomass

Table 10 List of designations.

No.	Designation	**Notes**
	1. Fluxes	
1	$[I]; I = [I]/ K^I$	Absolute and relative (in units of K^I) light (energy) flux
2	P_1^m	Absolute maximum specific rate of primary link
3	$V_1^m = P_1^m/P_1^m = 1/(r_{23} + r_3 + r_{34}) = 1$	Relative maximum specific rate of primary link
	$V_2^m = P_2^m/P_1^m = 1/(r_{56} + r_6) = 1/R_2$	Relative maximum specific rate of herbivore link
	$V_3^m = P_3^m/P_1^m = 1/(r_{78} + r_8) = 1/R_3$	Relative maximum specific rate of carnivore link
	$V_5^m = P_5^m/P_1^m = 1/(r_{90} + r_9) = 1/R_5$	Relative maximum specific rate of bacterial link
3	V_i, V_{ij}	Relative (to P_1^m) specific fluxes of ecosystem
4	$U_i = C_i * V_i; U_{ij} = C_i * V_{ij}; u_{ij} = C_i*v_{ij}$	Relative (to P_1^m) full fluxes of ecosystem
5	$P_i = V_i*P_1^m; P_{ij} = V_{ij}*P_1^m; p_{ij} = v_{ij}*P_1^m$	Absolute specific rate of i-th link
	2. Relative resistance **(*for specific fluxes*)**	
5	$r_{ci} = K^{Ci}/\Sigma[C_i]$	Incorporation or grazing of c_i-substrate (biomass) to (i+1)–th trophic link
6	$r_{ij} = P_1^m/\{k_{ij}*[E_i^0]*[E_j^0]\} = P_1^m/P^m_{ij}$	Coupling of substrate cycles with another cyclic reactions of link (capture resistance)
7	$r_i = P_i^m/(k_i*[E_i^0])$	Resistance substrate (food) processing of i-th link
8	$r_{i0} = P_1^m/k_{i0}$	Specific maintenance respiration of the expense of c_i-biomass
9	$r_{i4} = P_1^m/k_{i4};$	Specific rate of mortality
	3. Concentrations	
10	$[C_i];$ $\Sigma[C_i]$	Absolute concentration of i-th component (link) Total concentration of all components (links)
11	$C_i = [C_i]/\Sigma[C_i]$	Relative component concentrations
	4. Constants	
12	$K^I = P_1^m/(A*\varphi)$	Substrate constant for light energy
13	$K^{Ci} = P_i^m/(k_{ci}*[E_{ci}^0])$	Substrate constant for i-th substrate (biomass)
14	k_{i0}	Specific constant of maintenance respiration
15	$k_{i4}; k'_{i4}$	Specific constant of mortality 0-th and 1-th order respectively
	5. Coefficients	
16	α_i	Ecotrophic coefficient (food utilization efficiency) of i-th link
17	$\beta_i,$	Portion of captured food, using for biosynthesis respiration
18	γ_i	Portion of non-using food (excretion and egestion)

Table 11 Parameter values of six compartment ecosystem (Fig. 16, Table 9) which, to a considerable extent, correspond to parameter values for NEMURO Model (Eslinger *et al.* 2000).

No.	Parameter	Value	Notes
	1. Primary link		
1.1	$I = [I]/ K^I$	10	Relative (in units of K^I) light intensity
1.2	r_{c0}	0.2	Resistance of substrate uptake by primary link
1.3	P_1^m,	1,0 (1/day)	Absolute maximum specific rate of primary link
1.4	$V_1^m = P_1^m/P_1^m = 1/(r_{23} + r_3 + r_{34})$	1,0	Relative maximum specific rate of primary link
1.5	$r_{23} = r_{34}$	0.05	Resistance of reaction of coupling of substrate cycles with cycle of processing reactions
1.6	r3	0.9	Resistance of reactions of processing cycle
1.7	$R_1 = r_{23} + r_3 + r_{34}$	1.0	Total resistance of primary link
1.8	r_{10}	30	Resistance of specific maintenance respiration
1.9	r_{14}	100	Mortality
1.10	α	0.7	Growth efficiency
1.11	$\beta = \gamma$	0.15	Excretion and biosynthesis respiration
	2. Herbivorous (secondary) link		
2.1	r_{c1}	0.5	Resistance of substrate uptake (food grazing)
2.2	$V_2^m = P_2^m/P_1^m = 1/(r_{56} + r_6)$	1.0	Relative maximum specific rate of herbivore link
2.3	r_{56}	0.05	Resistance of coupling reaction of substrate (food) cycle with cycle of processing reactions
2.4	r_6	0.95	Resistance of reactions of processing cycle
2.5	$R_2 = r_{56} + r_6$	1.0	Total resistance of secondary link
2.6	r_{20}	25	Resistance of specific maintenance respiration
2.7	r_{24}	30	Mortality
2.8	$\alpha = \beta$	0.3	Growth efficiency and biosynthesis respiration
2.9	γ	0.4	Egestion
	3. Carnivorous link		
3.1	r_{c2}	1.0	Resistance of substrate uptake (food grazing)
3.2	$V_3^m = P_3^m/P_1^m = 1/(r_{78} + r_8)$	0.25	Relative maximum specific rate
3.3	r_{78}	0.2	Resistance of coupling reaction of substrate (food) cycle with cycle of processing reactions
3.4	r_8	3.8	Resistance of reactions of processing cycle
3.5	$R_3 = r_{78} + r_8$	4.0	Total resistance of carnivorous link
3.6	r_{30}	140	Resistance of specific maintenance respiration
3.7	r_{34}	100	Mortality
3.8	$\alpha = \beta$	0.3	Growth efficiency and biosynthesis respiration
3.9	γ	0.4	Egestion
	4. Bacterial link		
4.1	r_{c4}	0.08	Resistance of substrate uptake
4.2	$V_5^m = P_5^m/P_1^m = 1/(r_{90} + r_9)$	4.0	Relative maximum specific rate of bacterial link
4.3	r_{90}	0.0125	Resistance of coupling reaction of substrate cycle with cycle of processing reactions
4.4	r_9	0.2375	Resistance of reactions of processing cycle
4.5	$R_5 = r_{90} + r_{09}$	0.25	Total resistance of bacterial link
4.6	r_{50}	3.0	Resistance of specific maintenance respiration
4.7	r_{54}	10	Mortality
4.8	$\alpha = \beta$	0.3	Growth efficiency and biosynthesis respiration
4.9	γ	0.4	Egestion

	5. Concentrations		
5.1	$[C_i]$; $\Sigma[C_i]$	Not used	Absolute concentration of i-th component (link) Total concentration of all components (links)
5.2	$c_i = [C_i]/\Sigma[C_i]$	To be calculated	Relative component concentrations
5.3	$c_0 + c_1 + c_2 + c_3 + c_4 + c_5 = \Sigma\, c_i$	1.0	Total relative component concentrations

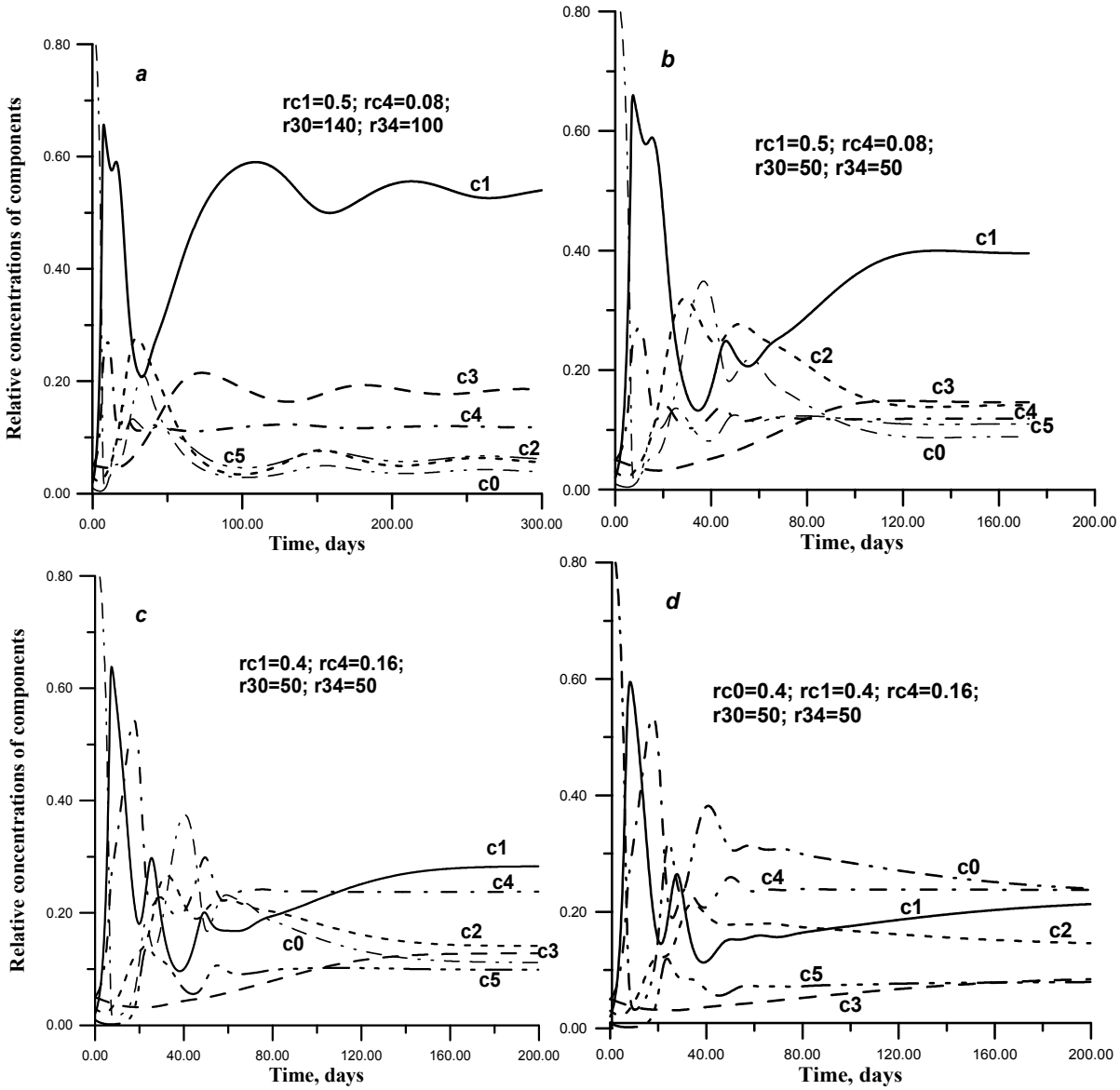

Fig. 17 Six compartment ecosystem model (Table 9)/TURBO PASCAL 7 output showing the time-dependence dynamics of concentrations of ecosystem components (link masses). The initial concentrations are: c1 = 0.02; c2 = 0.03; c3 = 0.05; c4 = 0.05; c5 = 0.01; c0 = 0.84 (phytoplankton, herbivores, carnivores, detritus, bacteria and inorganic matter correspondingly). a – parameters of Table 1; b – r30 and r34 decreased (spending of c3 increased); c – rc1 decreased and rc4 increased (substrate constant of c2 grazing to c1 increased and substrate constant uptake of c4 by c5 decreased); d – rc0 increased (substrate constant uptake of c0 by c1 decreased); and following on the next page, e – rc1 decreased (substrate constant of c2 grazing to c1 in addition); f – r23 increased and r3 decreased (in primary link), the dependence of primary production on nutrients is closed to Michaelis-Menten equation.

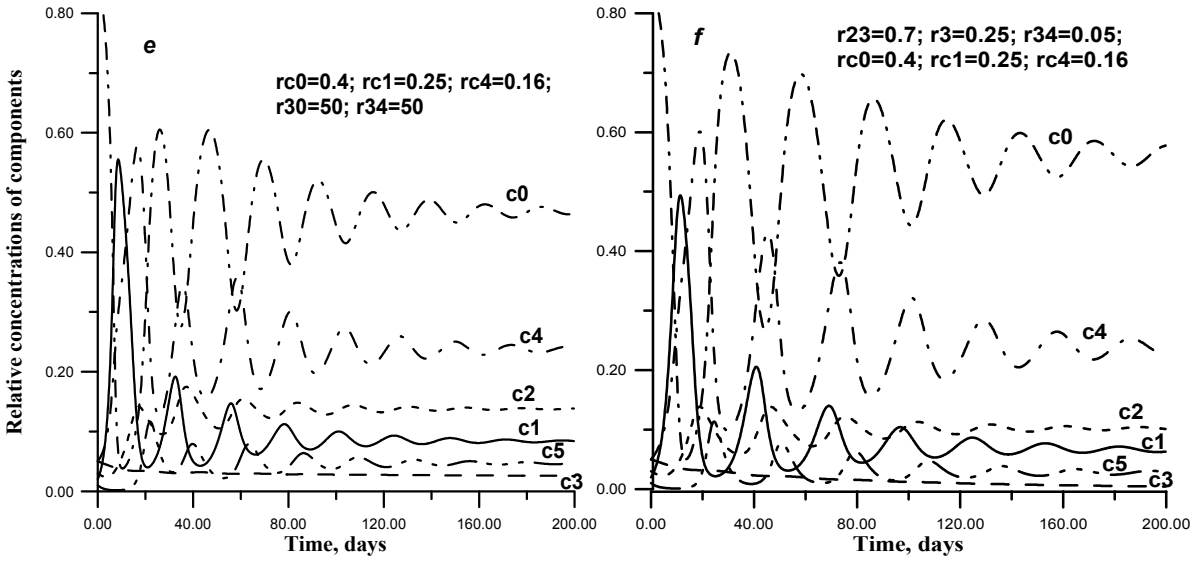

Fig. 17 (continued from the previous page)

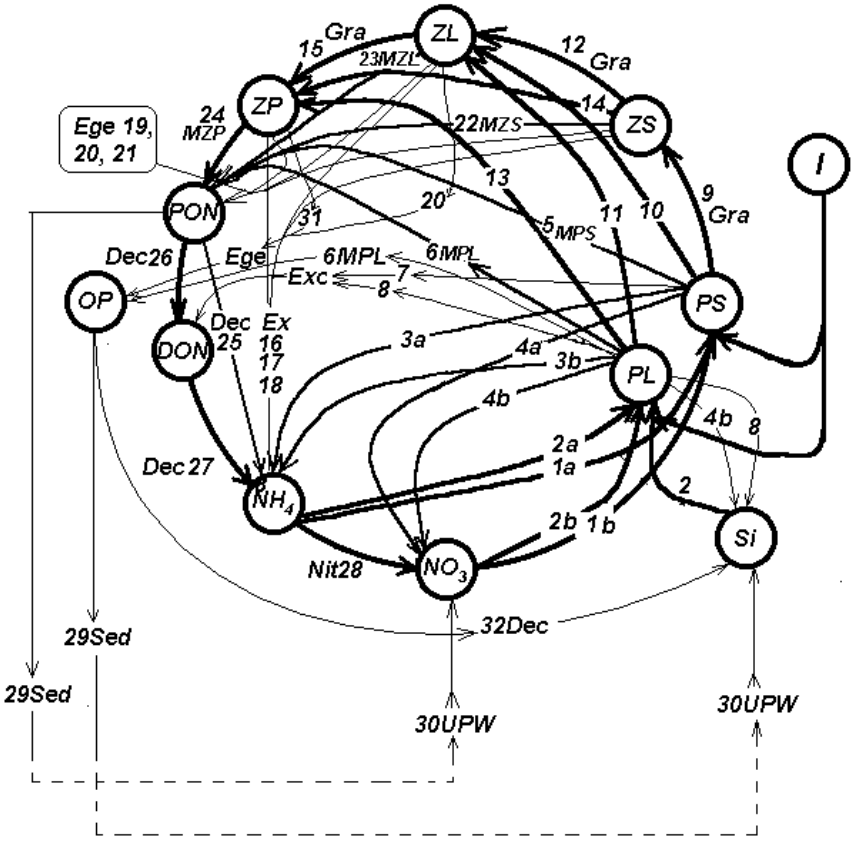

Fig. 18 NEMURO Model 2000, PICES CCCC prototype LTL marine ecosystem model. Ecosystem is represented as ecological cycle of limited nutrient. It is seen that cyclical flows of matter are the main attribute of ecosystem. Sedimentation and upwelling are the parts of the cyclical fluxes. Designation see in the original (Eslinger *et al.* 2000).

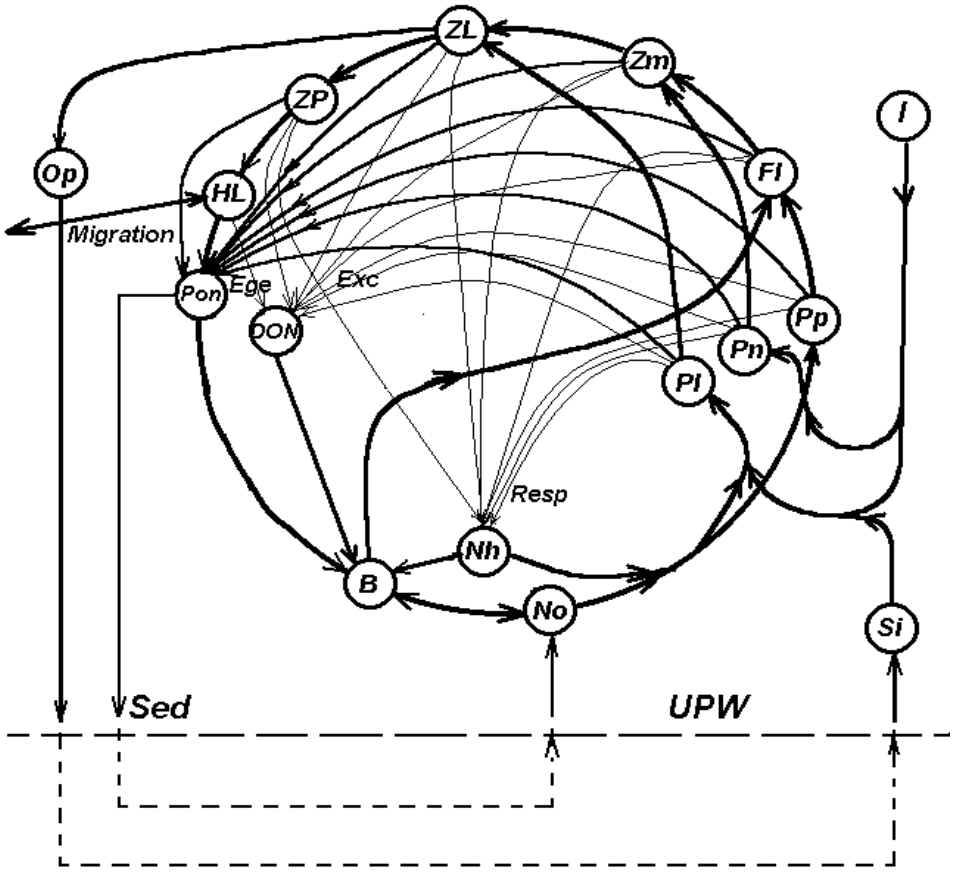

Fig. 19 The complicated NEMURO Model 2000. Model includes the microbial food web and higher trophic level (HTL). Such a model consists of 15 compartments. PON and DON are the food of bacteria with different preference; ammonium and nitrate are the sources of nitrogen. Bacteria in turn are the food to Flagellates (Fl). This model is describing by about of 60 algebraic and differential simultaneous equations. HTL can migrate in and off the ecosystem. Designation the same as in Figure 18.

Such relatively simple model as Figure 16 can be very convenient for investigation of ecosystem operation and its sensitivity to parameter changes. This model is the step to development and investigation of more complex ecosystem with including in it the bacterial and higher trophic levels (such as Fig. 19).

Figure 18 presents the NEMURO Model. This model can be complicated by way of including in it the bacterial food web and link of higher trophic level. Figure 19 presents the simplified variance of such a 15-compartment model. This model is described by a system of about 60 equations.

So the main difficulties lie in constructing the correct (close to reality) conceptual and mathematical models and in understanding its behavior. Which of the factors have a strong effect on ecosystem behavior and what other ones have a low influence on the system behavior needs to be established.

The unique approach, the possibility of composing the quantitative description of the schemes of arbitrary complexity gives the opportunity to apply it to all the processes in which the biological systems play significant part. We are sure that the proposed approach, based on the mechanism of biological processes, will allow us to describe and to understand both the functioning of each processes of the ecosystem, and the ecosystem as a whole. The results of our preliminary studies confirm such possibilities.

Coupling lower and higher trophic level models in marine ecosystems: Some considerations

Daniel M. Ware[1], Bernard A. Megrey[2], Francisco E. Werner[3] and Kenneth A. Rose[4]

[1] Adjunct-Professor, Department of Earth and Ocean Sciences, University of British Columbia. Mailing address: 3674 Planta Road, Nanaimo, B.C., Canada. V9T 1M2 E-mail: mandd@island.net

[2] National Marine Fisheries Service, Alaska Fisheries Science Center, 7600 Sand Point Way NE, Seattle, WA 98115, U.S.A. E-mail: bern.megrey@noaa.gov

[3] Marine Sciences Department, CB# 3300, University of North Carolina, Chapel Hill, NC 27599-3300, U.S.A. E-mail: cisco@email.unc.edu

[4] Coastal Fisheries Institute & Department of Oceanography and Coastal Sciences, Wetlands Resources Building, Louisiana State University, Baton Rouge, LA 70803, U.S.A. E-mail: karose@lsu.edu

The development of a coupled lower and higher trophic level model can be guided by asking five basic questions:

How many key functional groups link the lower and higher trophic levels?

Real food webs are very complex. Diet information can be used to determine the number of significant pathways linking LTL organisms to HTL predators. Seasonal changes in the diet also need to be considered. The model should have at least two pathways linking the lower and higher trophic levels; three is probably better and is certainly more realistic. Alternate pathways are important because they allow LTL production to flow at different rates, to different HTL predators, under different environmental conditions. Three globally important LTL linking groups are: copepods, euphausiids and predatory zooplankton. The order of importance of each of these groups can be expected to vary from place to place, and probably over time in response to climate regime shifts and anthropogenic impacts.

- Copepods are eaten by the larvae and juveniles of most higher trophic level fish species, and by all sizes of small pelagic fishes like herring, anchovy, sardine and sand lance.
- Euphausiids and predatory zooplankton are also eaten by a wide range of small and medium sized pelagic species (including mackerel and small hake).

For these reasons, the Task Team noted that consideration should be given to dividing the large zooplankton (ZL) component in the PICES NEMURO Model into separate copepod and euphausiid components.

What HTL response do we want to model and why?

Typically, the objective is to model the time-varying daily nutrient flux, and the biomass and production rates of key HTL predators, which are of commercial and societal importance, so the current state of these organisms and the resource management implications can be evaluated. Computationally, and also because of limited knowledge of some of the important biological processes, it is difficult to handle more than ten HTL species (or functional groups) in most dynamic models. An important exception to this is ECOSIM, which, because of the way it is structured, has the capability of handling up to fifty species. The number of species (or functional groups) that need to be included depends on the purpose of the model. A number of models of different complexity may be required to answer a range of species-specific questions.

How should each species or functional group of species be represented in the model?

The simplest arrangement is to have a single aggregated group (for example "small zooplankton" or "small pelagic fish"). In other cases, it may be more appropriate to structure the model so some of the key species are represented as a population of multiple size, or age groups. In all likelihood, the model will be structured with a mixture of simple, pooled functional groups, and one or more size or age structured species groups.

For example, the HTL model could contain a detailed age-specific sub-model of herring, with the other HTL predators aggregated into one or more functional groups, similar to the European Regional Sea Ecosystem Model (ERSEM).

How do HTL predators consume LTL production, or, what is the most likely functional response?

If predators and prey tend to be distributed uniformly in space then it is appropriate to use a simple prey-dependent type II functional response to model the feeding rate (I). Numerous short-term experiments have found that a type II functional response appears to characterize the feeding response of a variety of predators (e.g. Valiela 1995). However, experimental research has also shown that turbulent mixing, temperature, predator behaviour, and predator density can modify the functional response.

Mixing The rate of food consumption by fish larvae increases with the amount of turbulent mixing, because it increases the rate of prey contact (e.g. Sundby and Fossum 1990). Theoretically feeding rate increases with increasing turbulence, achieves a maximum at some intermediate turbulent mixing rate, after which feeding tapers off with increasing turbulence (Rothschild and Osborne 1988). This phenomenon is most important for small zooplankton and fish larvae, and perhaps some juvenile fish.

Temperature The rate of prey consumption and hence the maximum daily ration are dome-shaped functions of temperature (e.g. Brett and Groves 1979).

Predator behaviour Although rarer, there are examples of an S-shaped type III functional response (e.g. Valiela 1995). It may arise from changes in predator behaviour, like prey switching, or searching image formation.

Predator density If predators form dense schools, the resulting functional response will depend on both the predator (P) and prey (N) densities, in a manner that reflects feeding interference between the predators (Cosner *et al.* 1999). Accordingly, some of the more probable functional responses formulations include:

Holling Type II: Prey (N) dependent functional response (I is the ingestion rate) when the predator is uniformly distributed (Fig. 20).

$$I = eN / (1 + ehN)$$

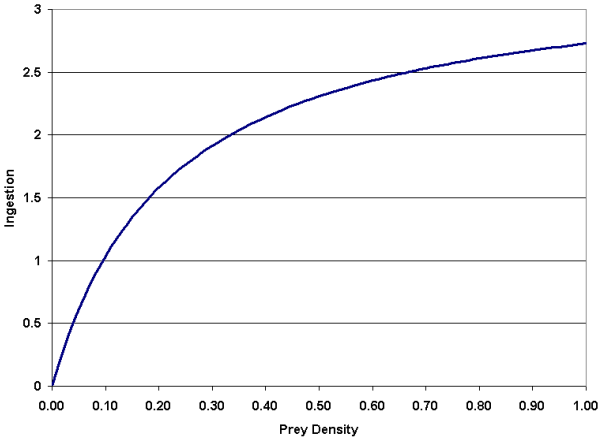

Fig. 20 Relationship between prey density and ingestion rate using a Holling II type functional response. Parameters used are e=15.0, h=0.3.

Holling Type III: S-shaped prey-dependent functional response (Fig. 21).

$$I = k / [1 + a \exp(-bN)]$$

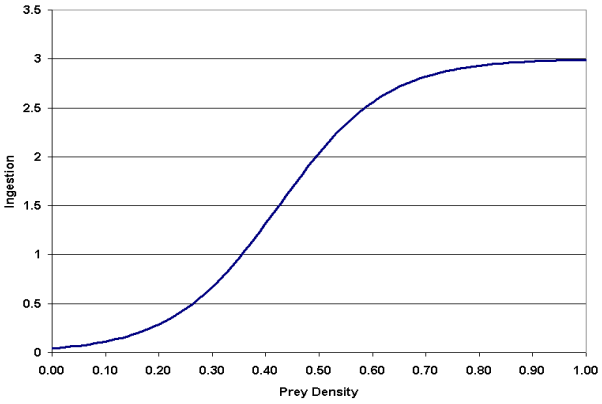

Fig. 21 Relationship between prey density and ingestion rate using a Holling III type functional response. Parameters used are k=3.0, a=70.0, and b=10.0.

Hassell-Varley Type: Functional response depends on both prey (N) and predator (P)

densities. For a school of predators foraging in 3 dimensions (Fig. 22):

$$I = ecN / (P^{1/3} + ehcN)$$

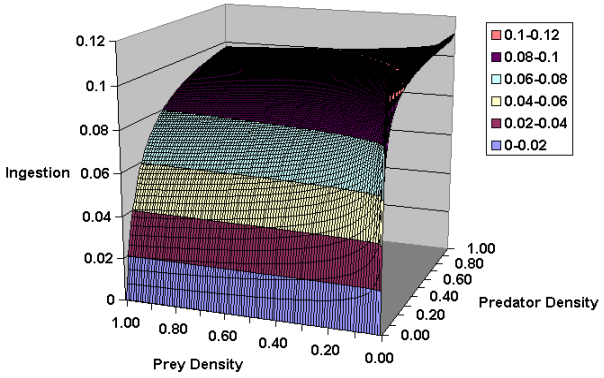

Fig. 22 Relationship between predator and prey density and ingestion rate using a Hassel-Varley type functional response. Parameters used are e=0.4, h=9.0, and c=2.0.

DeAngelis-Beddington Type: With feeding interference among predators (Fig. 23):

$$I = eP_oN / (P_o + P + ehP_oN)$$

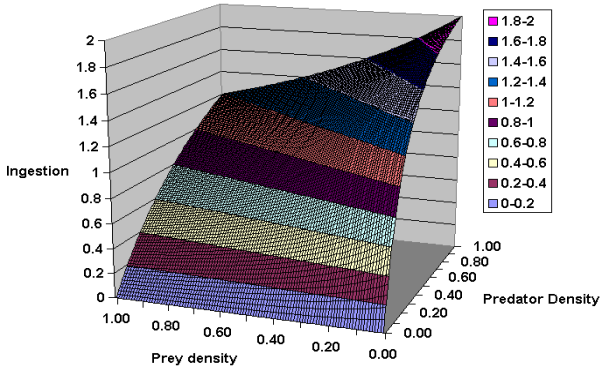

Fig. 23 Relationship between predator and prey density and ingestion rate using a De-Angelis-Beddington type functional response. Parameters used are e=10.0, h=0.4 and P_0=0.3.

How much consumed energy is converted into HTL predator production?

Three important factors affecting HTL predator growth rates are the size of the food ration, the metabolic rate, and water temperature.

The master bioenergetics equation is:

$$I = E + M + G$$

where I = ingested energy, E = excretion, M = metabolism, and G = growth (and reproduction). For well-fed carnivorous fish in the laboratory Brett and Groves (1979) found:

$$(100)I = (27)E + (44)M + (29)G$$

In natural ecosystems, E will probably be similar, but M will be much higher because of the additional metabolic costs incurred by finding food and avoiding predators, and because natural foods are not as digestible as the man-made foods that were used in these experiments. Hence G will be much lower, probably around 10% to 15% of the ingested ration.

- The growth rate is usually a saturating function of ration size (Brett *et al.* 1969), but in some cases it may be weakly dome-shaped at very high rations.
- The growth efficiency tends to be highest at intermediate sized rations (Brett *et al.* 1969).
- For any given ration, the resulting growth rate is a dome-shaped function of temperature (Brett *et al.* 1969). In Figure 24, note how the highest growth rate occurs at a lower temperature when the prey density, and hence the ration, are reduced. This is an important phenomenon, which the HTL component of the model should be able to reproduce.

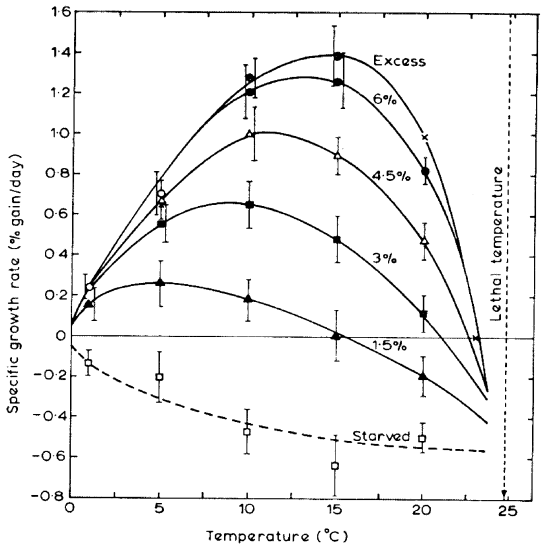

Fig. 24 Relation between temperature and specific growth rate (± 2 S.E.) of young *Orcorhynchus nerka* when fed various rations as percentage of body dry weight. Points marked (X) and (O) are separate experiments using excess ration (after Brett *et al*. 1969).

Are seasonal migrations by HTL predators important?

Large biomasses of fish, birds and marine mammals migrate into or through most subarctic marine ecosystems in the summer to feed.

- The arrival time and the biomass of these migrants can have a significant impact on the biomass and production of LTL prey species. (e.g. Robinson and Ware 1994).
- The largest fish tend to migrate further north (e.g. sardine and hake in the NE Pacific).
- Presumably the movements of migrating species are also affected by other factors like: temperature, food supply, predators, reproductive state, etc. Much more needs to be learned about this.

Diagnostic analysis

Once the coupled model has been constructed and the output has passed a "reasonableness" test the model can be used as a tool to diagnose the current productivity of the system. Time series measurements of important physical variables, like radiation, temperature, and wind speeds, and the estimated biomass of important fish species (from stock assessment analyses), can be input to the model to estimate the *current lower trophic level productivity* of the system, and the productivity of some key HTL organisms. The results will enable fisheries managers to determine if the target harvest rates are sustainable. This information will be very useful, because it will enable the manager to adjust the harvest rate annually, in response to model estimates of the current productivity of the system.

Prognostic analysis

Prognostic analysis is very difficult because it involves predicting the future state of complex ecosystems. For successful long-range forecasting we need to be able to estimate how the future growth, mortality and recruitment rates of each key species in the model will respond to both "bottom-up" forced and "top-down" forced changes in the state of the system. These changes are caused by natural variations in the physical forcing variables and by anthropogenic forcing, through global warming, habitat destruction and over-fishing. Given our current, limited knowledge about many of the complex processes involved here, long-range productivity forecasting cannot be done with any precision at this time. Accordingly, the production of most HTL species should not be forecast more than a few years ahead, until the models improve.

An overview of ECOPATH/ ECOSIM

Steven J.D. Martell
Fisheries Centre, University of British Columbia, Vancouver, B.C., Canada. V6T 1Z4 E-mail: smartell@fisheries.com

A brief overview of the ECOPATH/ECOSIM modeling approach was provided in request of the potential need to couple the NEMURO model to another higher trophic level modeling paradigm.

A tool for visualizing ecosystem model output

Kerim Y. Aydin
National Marine Fisheries Service, Alaska Fisheries Science Center, 7600 Sand Point Way NE, Seattle, WA 98115, U.S.A. E-mail: kerim.aydin@noaa.gov

A demonstration was given of a custom software that assists visualizing ecosystem model output. The tool organizes output information by trophic level and plots fluxes as a ration of production to biomass. Figure 25 shows an example screen shot from an eastern tropical Pacific tuna fishery.

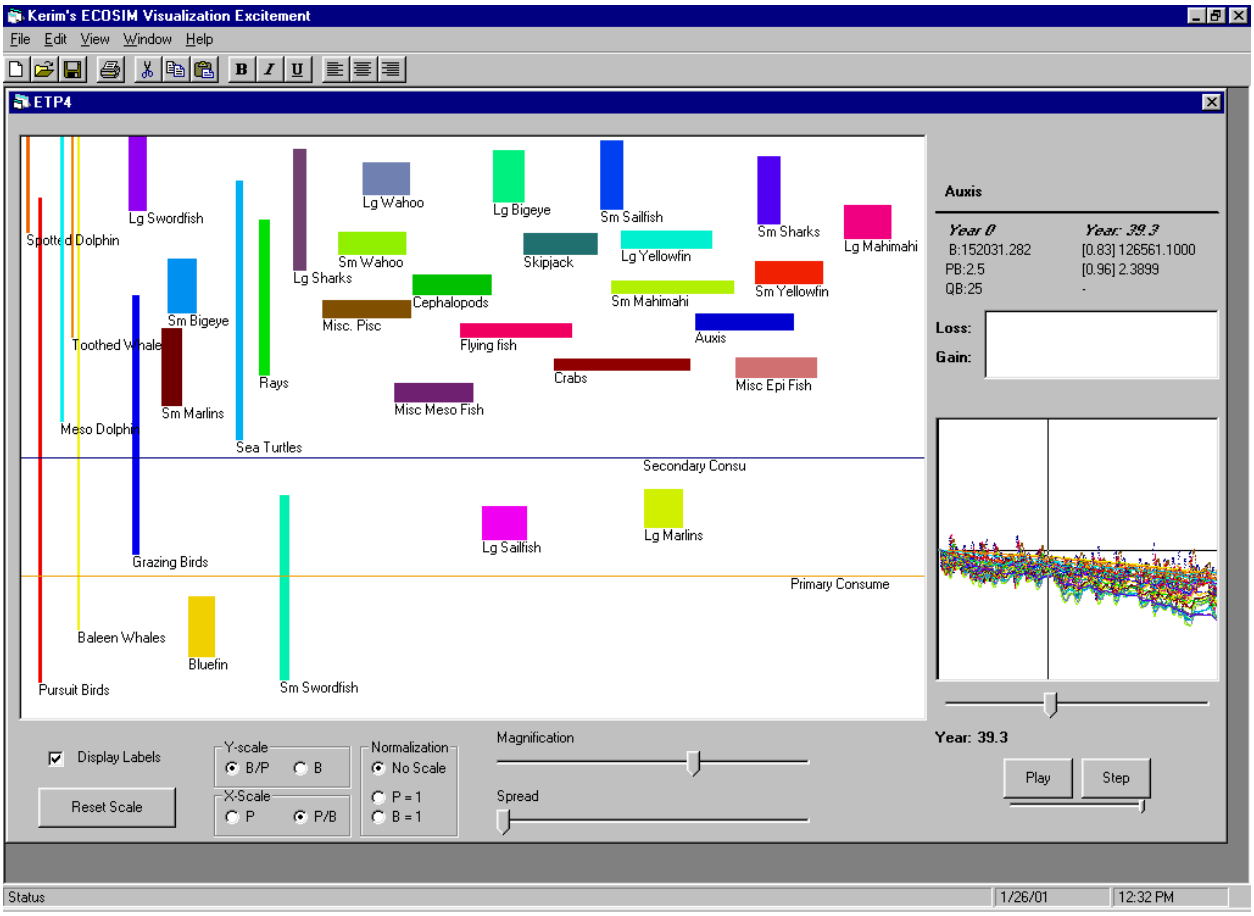

Fig. 25 Example of prototype NEMURO visualization software. Example presented is a simulation of the eastern tropical Pacific tuna fishery, showing the relative Biomass (Y-dimension of each box) and P/B ratio (X-dimension of each box) during a period of high production. R-selected species have long horizontal direction, while K-selected species have a long vertical direction.

MODEL Workshop Summary

At the Hakodate Workshop, the MODEL Task Team discussed some of the processes that need to be considered for representing LTL coupled to HTL trophodynamics in marine ecosystems. The Task Team noted that significant advances in modeling the dynamics of LTL in aquatic systems (i.e. the microbial food web, and large phytoplankton and zooplankton) have occurred in the last decade. Progress has also been made in linking the production of HTL organisms (e.g. squid, fish, seabirds, and marine mammals) to LTL production models. Problems still exist when scaling process information and data to the scales required for marine ecosystem models. Figure 26 (ICES Study Group 1993) summarizes the relationship between observed species composition, state variables in modeling approaches that build from the "bottom up" with increasing complexity (and numbers of species). The suggested approach is to focus on the target species with links to lower and higher trophic levels by aggregating/sub grid-scale representation rather than including the full complexity of the neighboring trophic components.

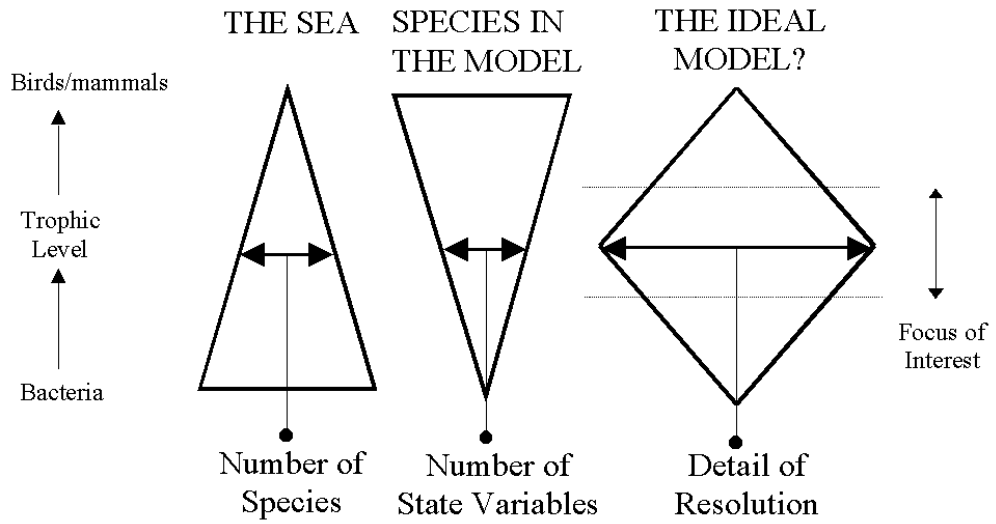

Fig. 26 Cartoon depicting tradeoffs between spatial and temporal scales of model resolution and model integration as they relate to modeling ecosystems. After ICES Study Group on Spatial and Temporal Integration, Glasgow, 1993 (ICES C.M. 1993/L:9).

Since LTL and HTL organisms function on different time and spatial scales within the ecosystem, successful coupling requires getting a number of things right -- or just about right. In this context, information about the diet, the functional response, growth efficiencies, large-scale seasonal movements of migratory species, and the impact of climate variability on these processes are required. For some marine ecosystems in the PICES area, enough biological, ecological, and stock assessment knowledge exists to begin using coupled models as primitive diagnostic tools to assess the current productivity and impacts of climate change on the ecosystem, and the effects on the dynamics of the key organisms within it. The development of a successful prognostic capability is a more challenging, longer-term problem, which requires getting a number of other things right, such as recruitment dynamics, dispersal and migratory behavior, and behavioral changes in predator-prey interactions.

Recommendations

- Convene a MODEL Workshop to implement improvements to the PICES NEMURO model.
- Increase interaction with BASS and REX to support their modeling initiatives through cooperative modeling workshops.
- The CCCC Co-Chairmen should present these workshop proposals to the Science Board as a coordinated package of integrated activity underscoring the cooperation and interdependencies.
- Facilitate joint planning; time needs to be allocated at the next PICES Annual Meetings for joint CCCC inter-sessional meetings.
- Encourage opportunities for more CCCC Task Team interaction, joint CCCC Task Team meetings are needed to coordinate and implement Task Team plans. In Victoria, the Task Team meetings should be at non-overlapping times and places.
- Request that the PICES Secretariat provide assistance to help MODEL build a web page to present NEMURO code, data and results.
- Issues related to model management need to be addressed so as to better control the increasing number of different versions of a model, including process equations, parameter files, physical forcing data files, and post processing programs. We propose to examine the ICES/GLOBEC experience to obtain guidance as to how best to proceed.
- Develop "NEMURO/Stella" Box Model using the Stella software package.
- Make progress on preparing an executable version of the prototype model available on the WWW.

- Develop a means of staying in contact to continue unfinished work.

Achievements and future steps

- Link with high trophic level model.
- The LTL model needs to include fishes, marine mammal, marine birds, and also micro-nekton.
- Perform basic model validation studies.
- Develop model validation protocols.
- Compare physical factors with direct observations.
- Compare model biomass predictions with direct observations at Stations A7 and the Bering Sea.
- Identify scientific questions for comparison.
- Communication and cooperation with the REX and BASS Task Teams is needed.
- Perform listed experiments.
- NEMURO extensions:
  - add Fe limitation to phytoplankton production;
  - add microbial food web;
  - split ZL into copepods and euphausiids;
  - add sinking rate of phytoplankton to detritus pool;
  - parameterize NEMURO to a coastal region.
- NEMURO diagnostics:
  - code diagnostic and performance measures into NEMURO such as P/B, C/B ratios and ecotrophic efficiency calculations;
  - validate model output against data fro each regional location;
  - perform side-by-side comparison of NEMURO Box and NEMURO MATLAB models to same equations and data.
- Spatially explicit approach:
  - extend 1-D coupled model per above;
  - work toward eventually embedding NEMURO into larger scale 3-D ocean model similar to Kawamiya *et al.* (2000a, 2000b).
- Linkages with other CCCC components:
  - modify NEMURO per needs of REX and convene joint workshop to achieve extension of NEMURO to include higher trophic levels;
  - devise scheme to link NEMURO with ECOPATH/ECOSIM with the aim towards meeting the objectives of BASS.
- Establish links with other programs such as GODAE, WCRP, CLIVAR.
- Modifications as required to accommodate BASS and REX needs.

References

Brett, J.R., Shelbourn, J.E., and Shoop, C.T. 1969. Growth rate and body composition of fingerling sockeye salmon, *Oncorhynchus nerka* , in relation to temperature and ration size. Journal of the Fisheries Research Board of Canada 26: 2363-2394.

Brett, J.R., and Groves, T.D. 1979. Physiological energetics. *In* Fish Physiology Vol. VIII. Academic Press. P. 280-352.

Cosner, C., DeAngelis, D.L., Ault, J.S., and Olson, D.B. 1999. Effects of spatial grouping on the functional response of predators. Theoretical Population Biology 56: 65-75.

DeAngelis, D.L., Rose, K.A., Crowder, L., Marschall, E., and Lika, D. 1993. Fish cohort dynamics: application of complementary modeling approaches. American Naturalist 142: 604-622.

Edwards, G., and Walker, D. 1983. C3, C4 : mechanisms, and cellular and environmental regulation, of photosynthesis. Oxford, Blackwell Scientific Publications: 598 p.

Eslinger, D.L., Kashiwai, M.B., Kishi, M.J., Megrey, B.A., Ware, D.M., and Werner, F.E. 2000. Final report of the International Workshop to Develop a prototype lower trophic level ecosystem model for comparison of different marine ecosystems in the North Pacific. *In* PICES-GLOBEC International Program on Climate and Change and Carrying Capacity Report on the 1999 MONITOR and REX Workshops, and the 2000 MODEL Workshop on Lower Trophic Level Modeling. *Edited by* B.A. Megrey, B.A. Taft, and W.T. Peterson. PICES Scientific Report No. 15, 285p.

Falkowski, P.G., and Wilson, C. 1992. Phytoplankton productivity in the North Pacific since 1900 and implications for absorption of anthropogenic CO2. Nature. 358: 741-743.

Fasham M.J.R. 1995. Variations in the seasonal cycle of biological production in subarctic oceans: a model sensitivity analysis. Deep-Sea Research I. 42: 1111-1149.

Fasham, M.J.R., Ducklow, H.W., and McKelvie, D.S. 1990. A nitrogen-based model of plankton dynamics in the oceanic mixed layer. Journal of Marine Research 48: 591-639.

Goodwin, T.W., and Mercer, E.I. 1983. Introduction to Plant Biochemistry. Oxford, Pergamon Press, Vol. 1: 392p.

Hinckley, S. 1999. Biophysical mechanisms underlying the recruitment process in walleye pollock (*Theragra chalcogramma*). Ph.D. Dissertation. University of Washington, Seattle. 259p.

ICES Study Group on Spatial and Temporal Inte-gration, Glasgow, 1993 (ICES.C.M. 1993/L:9)

Kawamiya, M, Kishi, M.J., Yamanaka, Y., and Suginohara, N. 1995. An ecological-physical coupled model applied to Station P. Journal of Oceanography 51: 635-664.

Kawamiya, M., Kishi, M.J., Yamanaka, Y., and Suginorhara, N. 1997. Obtaining reasonable results in different oceanic regimes with the same ecological-physical coupled model. Journal of Oceanography 53: 397-402.

Kawamiya, M., Kishi, M.J., and Suginohara, N. 2000a. An ecosystem model for the North Pacific embedded in a general circulation model. Part I: Model description and characteristics of spatial distributions of biological variables. Journal of Marine Systems 25: 129-157.

Kawamiya, M., Kishi, M.J., and Suginohara, N. 2000b. An ecosystem model for the North Pacific embedded in a general circulation model. Part II: Mechanisms forming seasonal variations of chlorophyll. Journal of Marine Systems 25: 159-178.

Kishi, M.J., Motono, H., Kashiwai, M., and Tsuda, A. 2001. An ecological-physical coupled model with ontogenetic vertical migration of zooplankton in the northwestern Pacific. Journal of Oceanography (submitted).

Longhurst, A., Sathyendranath, A., Platt, T., and Caverhill, C. 1995. An estimate of global primary production in the ocean from satellite radiometer data. Journal of Plankton Research 17: 1245-1271.

Megrey, B.A., Kishi, M.J., Kashawai, M.B., Ware, D., Werner, F.E., and Eslinger, D.L. 2000. PICES Lower Trophic Level Modeling Workshop, Nemuro 2000. PICES Press 8: 18-22.

Oguz, T., Ducklow, H.W., Malanotte-Rizzoli, P., Murray, J., Shushkina, E.A., Vedernikov, V.I., and Unluata, U. 1999. A physical-biochemical model of plankton productivity and nitrogen cycling in the Black Sea. Deep-Sea Research 46: 597-636.

Platt T., Denman, K.L., and Jassby, A.D. 1977. Modelling the productivity of phytoplankton. *In* The sea: ideas and observations of progress in the study of the seas, Vol. 6. *Edited by* E.D.Goldberg, I.N.McCave, J.J.O'Brien and J.H.Steele. New York, N.Y., John Wiley & Sons pp. 807-856.

Robinson, C.L.K., and Ware, D.M. 1994. Modeling pelagic fish and plankton trophodynamics off southwestern Vancouver Island, British Columbia. Can. J. Fisheries and Aquatic Sciences 51: 1737-1751.

Rose, K.A. 2000. Why are quantitative relationships between environmental quality and fish populations so elusive? Ecological Applications 10: 367-385.

Rothschild, B.R., and Osborn, T.R. 1988. Small-scale turbulence and plankton contact rates. Journal of Plankton Research 10: 465-474.

Straile, D. 1997. Gross growth efficiencies of protozoan and metazoan zooplankton and their dependence on food concentration, predator-prey weight ratios, and taxonomic group. Limnol. Oceanogr. 42: 1375-1385.

Shiotani, T., and Uye, S. 2000. Selective feeding of the calanoid copepod *Calanus sinicus* on the natural microplankton assemblage, with special reference to microzooplankton. Abstracts. PICES Ninth Annual Meeting. Hakodate. pp. 133-134.

Sundby, S., and Fossum, P. 1990. Feeding conditions of Arctro-norwegian cod larvae compared with the Rothschild-Osborn theory on small-scale turbulence and plankton contact rates. J. Plankton Res. 12: 1153-1162.

Steele, J.H. 1962. Environmental control of photosynthesis in the sea. Limnol. Oceanogr. 7: 137-150.

Valiela, I. 1995. Marine ecological processes. Springer-Verlag New York. 686p.

Wang, S-B. 1998. Comparative studies of the life history and production potential of bay anchovy *Anchoa mitchilli* and northern anchovy *Engraulis mordax*: an individual-based modeling approach. Ph.D. Dissertation. University of South Alabama, Mobile.

Wong, C.S., Whitney, F.A., Iseki, K., Page, J.S., and Zeng, J. 1995. Analysis of trends in primary productivity and chlorophyll-a over two decades at Ocean Station P (50° N 145° W) in the Subarctic Northeast Pacific Ocean. *In* Climate Change and Northern Fish Populations. *Edited by* R.J. Beamish. Canadian Special Publication in Fisheries and Aquatic Sciences 121: 107-117.

Zvalinsky, V.I., and Litvin, F.F. 1986. Steady-state kinetics of chains of coupled cyclic reactions. Biochimiya (Rus.) 51: 1741-1755.

Zvalinsky, V.I., and Litvin, F.F. 1988a. Modelling of photosynthesis and its coupled processes. Biofisika (Rus.) 33: 169-182.

Zvalinsky, V.I., and Litvin, F.F. 1988b. The photosynthesis dependence on carbon concentration, intensity and spectral composition of light. Fisiologiya rastenii (Rus.) 35: 444-457.

Zvalinsky, V.I., and Litvin, F.F. 1991. Quantitative analysis of photosynthesis adaptation to light. Fisiologiya rastenii (Rus.) 38: 431-442.

MODEL Endnote 1

Participation List

Canada
- Kenneth L. Denman
- Steven J. Martell
- Daniel M. Ware

Japan
- Michio J. Kishi
- Hiroshi Kuroda
- Maki Noguchi
- Masako Saitoh
- Lan S. Smith
- Yasuhiro Yamanaka

Korea
- Sukyung Kang

Russia
- Gennady A. Kantakov
- Vladimir I. Zvalinsky

U.S.A.
- Kerim Y. Aydin
- Andrew W. Leising
- Sarah Hinckley
- Bernard A. Megrey
- Kenneth A. Rose
- Francisco E. Werner

Other
- Sergio Hernandez (Mexico)

MODEL Endnote 2

Meeting Schedule

Friday, October 20, 2000

CCCC First Plenary Session

09:25-09:35 Overview of MODEL workshop and activities (Kishi & Megrey)

11:00-11:30 Kenneth A. Rose. (keynote speaker) A review of the use of individual-based models as upper trophic level modelling tools.

MODEL Workshop

13:30-13:45 Opening remarks (Kishi)

13:45-14:15 Bernard A. Megrey, M.J. Kishi, D.M. Ware and M. Kashiwai. Summary of NEMURO 2000: An international workshop to develop a prototype lower trophic level ecosystem model for comparison of different marine ecosystems in the North Pacific.

14:15-14:35 Michio J. Kishi and H. Kuroda. Sensitivity analysis on NEMURO.

14:35-14:55 Vadim V. Navrotsky. To the physical forcing and the ways of improvements in the NEMURO model.

14:55-15:15 Francisco E. Werner and D.L. Eslinger. Lower trophic level models in oceanic ecosystems: status of the NEMURO LTL model and suggested extensions.

15:15-15:35 Yasuhiro Yamanaka, N. Yoshie, M. Fujii and M.J. Kishi. NEMURO model follow up.

15:35-15:55 Coffee/tea Break

15:55-16:15 Vladimir I. Zvalinsky. Coupling of different trophic levels in marine ecosystem models.

16:15-16:35 Daniel M. Ware. Coupling lower and higher trophic level models in marine ecosystems: an overview.

16:35-17:30 Discussion

Saturday, October 21, 2000

MODEL Workshop

09:00-09:30 Steven J. Martell. Review on ECOPATH modeling.

09:30-09:50 Fransisco E. Werner. Report from GLOBEC Focus 3 WG.

09:50-10:40 Discussion how to connect lower trophic and higher trophic level models (Discussion leaders: Kishi & Megrey)

10:40-11:00 Coffee/tea Break

11:00-12:00 Discussion how to connect lower trophic and higher trophic level models (Discussion leaders: Megrey & Kishi)

12:00-13:00 Future work and recommendations

CCCC Second Plenary Session

14:15-14:30 Report of MODEL Workshop and recommendations (Megrey)